IEEE Access
Multidisciplinary ⋮ Rapid Review ⋮ Open Access Journal

Received 21 July 2022, accepted 10 August 2022, date of publication 18 August 2022, date of current version 25 August 2022.

Digital Object Identifier 10.1109/ACCESS.2022.3199759

RESEARCH ARTICLE

General Analysis of a Loop Antenna Located on a Uniaxial Metamaterial Cylinder

ANNA S. ZAITSEVA[1], **ALEXANDER V. KUDRIN**[1], **AND TATYANA M. ZABORONKOVA**[1,2]

[1]Department of Radiophysics, University of Nizhny Novgorod, 603022 Nizhny Novgorod, Russia
[2]Department of Nuclear Physics, R. E. Alekseev Technical University of Nizhny Novgorod, 603950 Nizhny Novgorod, Russia

Corresponding author: Anna S. Zaitseva (zaitseva@rf.unn.ru)

This work was supported in part by the Russian Science Foundation (in the part related to the antenna analysis) under Project 21-72-00101, and in part by the Ministry of Science and Higher Education of the Russian Federation (in the part related to the study of modes of a metamaterial cylinder) under Project 0729-2020-0040.

ABSTRACT The general problem of determining the electrodynamic characteristics of a circular loop antenna located coaxially on the surface of a metamaterial cylinder is studied using the integral equation method. The antenna has the form of a perfectly conducting, infinitesimally thin, narrow strip coiled into a ring and is excited by a given time-harmonic voltage. The cylinder is assumed to be filled with a uniaxial metamaterial and surrounded by an isotropic magnetodielectric. Integral equations for azimuthal harmonics of the antenna current are derived and solved in the cases where the normal waves of the metamaterial inside the cylinder have either hyperbolic or nonhyperbolic dispersion. Based on the solutions of these equations, the current distribution and input impedance of the antenna are found in closed form. The behavior of the antenna characteristics as functions of the metamaterial parameters is discussed.

INDEX TERMS Current distribution, input impedance, integral equations, loop antenna, uniaxial metamaterial.

I. INTRODUCTION

Electromagnetic phenomena occurring in the presence of metamaterials have attracted much interest over the past decades (see, e.g., [1], [2], [3], [4], [5], and references therein). In particular, a great deal of attention has been paid to various guiding systems based on metamaterials, including the excitation and propagation of electromagnetic waves in such systems [5], [6], [7], [8], [9], [10]. For these applications, both volume metamaterial structures and metasurfaces have extensively been considered [11], [12]. The interest in the subject has largely been stimulated by the progress in creating new artificial media whose material parameters differ significantly from those of conventional media. The unusual properties demonstrated by metamaterials may lead to some unexpected behaviors of the characteristics of electromagnetic sources operated in the vicinity or on the surface of metamaterials [13], [14], [15], [16], [17], [18], [19], [20], [21], [22], [23]. In this respect, the use of metamaterial substrates in antenna devices becomes especially attractive.

In most works dealing with antennas located on metamaterial substrates, current distributions in the antennas are assumed given. This assumption, which is common for antennas that are electrically sufficiently small, cannot be used if electromagnetic sources are located on the surface of or inside a hyperbolic metamaterial. In such a material, potential (electrostatic or magnetostatic) propagating waves with infinitesimally short wavelengths are known to exist [4], [5], [18], in terms of which even a physically small antenna appears to be electrically large and, similarly, the antenna wire, no matter how thin it is, becomes indefinitely thick. Since most metamaterials, including the hyperbolic ones, are anisotropic, the methods available for antennas located on the surface of conventional anisotropic media can be applied in this case, with appropriate extension to hyperbolic dispersion when required [24], [25], [26], [27].

The antenna analyses which are referred to in the above have primarily focused on strip antennas located at a plane interface between anisotropic and isotropic media. Of no less

The associate editor coordinating the review of this manuscript and approving it for publication was Tutku Karacolak.

interest is the case where strip antennas are placed on the cylinder filled with an anisotropic metamaterial. Depending on the metamaterial parameters, such a cylinder can support eigenmodes of various types, and this circumstance may significantly affect the performance of antennas. Thus, accurate characterization and design of such antenna devices must account for this effect.

Note that the current distribution and input impedance of a loop antenna placed at a cylindrical interface between an anisotropic plasma and an isotropic medium have already been considered in [28] and [29]. At the same time there has been little effort in this direction for antennas located on a cylinder filled with an anisotropic metamaterial. In the cases where the anisotropic material of the cylinder is described by the dielectric permittivity or magnetic permeability tensor, this problem has separately been considered in [30] and [31]. However, for metamaterials that simultaneously possess both dielectric and magnetic anisotropy, the earlier obtained solutions require a corresponding generalization. Although such an attempt has recently been made in our preliminary study for one particular combination of the metamaterial parameters [32], the problem is still far from complete.

The present article thus treats the problem of the current distribution and input impedance of a circular loop antenna located coaxially on the surface of a cylinder filled with a uniaxial anisotropic metamaterial whose dielectric permittivity and magnetic permeability are described by diagonal tensors. We will consider all possible cases that can occur when using such tensors, assuming that the outer medium outside the cylinder is an isotropic magnetodielectric with scalar permittivity and permeability. The emphasis here is placed on employing the analytical approach as fully as possible, although some comparison of the analytical and numerical solutions will also be given. This is explained by not only obvious advantages of closed-form analytical results over purely numerical ones but also the desire to reveal the physical factors determining the antenna characteristics as functions of the problem parameters.

To obtain the antenna characteristics, one should first derive a formal representation of the electromagnetic field excited by the antenna. Since no closed-form expressions of the Green's functions exist for the cylindrical geometry discussed herein, we will employ the Fourier transform technique to describe the antenna field. While it is possible to deal with the field representation yielded by this approach, it turns out that it is actually simpler to pass from the Fourier transforms of the fields to their eigenfunction expansions in the resultant integral equation formulation. It is done below to find a closed-form solution for the antenna current distribution.

Our article is organized as follows. In Section II, we formulate the problem and describe the theoretical model. Section III deals with the derivation of integral equations for the azimuthal harmonics of the antenna current. The kernels of the integral equations are analyzed in Section IV. Section V presents an analytical solution for the current distribution of the antenna, its input impedance, and the numerical results for these characteristics. The conclusions following from the performed analysis are summarized in Section VI. Some auxiliary mathematical derivations and certain properties of eigenmodes supported by the metamaterial cylinder are discussed in the appendixes.

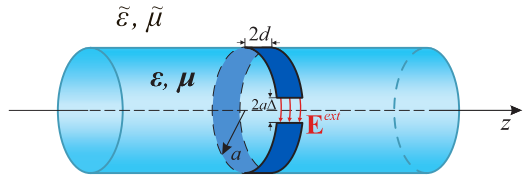

FIGURE 1. Geometry of the problem.

II. THEORETICAL MODEL AND BASIC EQUATIONS

Consider an antenna in the form of a perfectly conducting, infinitesimally thin, narrow strip of half-width d, which is coiled into a circular loop of radius a such that $a \gg d$. The antenna is located coaxially on the surface of an infinitely long cylinder which is aligned with the z-axis of a cylindrical coordinate system (ρ, ϕ, z) and surrounded by a homogeneous magnetodielectric medium with the dielectric permittivity $\tilde{\varepsilon} = \epsilon_0\varepsilon$ and the magnetic permeability $\tilde{\mu} = \mu_0\mu$ (see Fig. 1). Here, ϵ_0 and μ_0 are the permittivity and permeability of free space, respectively, and ε and μ are certain constants. The medium inside the cylinder is assumed homogeneous and describable by the permittivity tensor

$$\boldsymbol{\varepsilon} = \epsilon_0 \begin{pmatrix} \varepsilon_\perp & 0 & 0 \\ 0 & \varepsilon_\perp & 0 \\ 0 & 0 & \varepsilon_\parallel \end{pmatrix} \quad (1)$$

and the permeability tensor

$$\boldsymbol{\mu} = \mu_0 \begin{pmatrix} \mu_\perp & 0 & 0 \\ 0 & \mu_\perp & 0 \\ 0 & 0 & \mu_\parallel \end{pmatrix}. \quad (2)$$

The anisotropy axis of the metamaterial is thus parallel to the z-axis. The elements of the tensors in (1) and (2) depend on a particular type of metamaterial [33]. Throughout this article, all media are considered lossless.

Assuming a suppressed $\exp(+j\omega t)$ harmonic time dependence of an external voltage supplied to a narrow excitation gap $|\phi - \phi_0| \leq \Delta \ll \pi$ of the antenna, an electric field with a single nonzero component E_ϕ^{ext} at $\rho = a$ and $|z| < d$, which corresponds to this voltage, can be written in the form

$$E_\phi^{ext}(a, \phi, z) = \frac{V_0}{2a\Delta}[U(\phi - \phi_0 + \Delta) - U(\phi - \phi_0 - \Delta)] \times [U(z + d) - U(z - d)]. \quad (3)$$

Here, V_0 is the amplitude of the voltage supplied to the excitation gap centered at $\phi = \phi_0$, Δ is the angular half-width of this gap, and U is the Heaviside function. The distribution of E_ϕ^{ext} for $|z| < d$ can be represented as

$$E_\phi^{ext} = \sum_{m=-\infty}^{\infty} \mathcal{E}_m \exp(-jm\phi) \tag{4}$$

where m is the azimuthal index ($m = 0, \pm 1, \pm 2, \ldots$) and

$$\mathcal{E}_m = \frac{V_0}{2\pi a} \frac{\sin(m\Delta)}{m\Delta} \exp(jm\phi_0). \tag{5}$$

The density $\mathbf{J}$ of the electric current, which is excited in the antenna by the external field (3), can be sought in the form

$$\mathbf{J}(\rho, \phi, z) = \hat{\boldsymbol{\phi}}_0 I(\phi, z)\delta(\rho - a) \tag{6}$$

where $\hat{\boldsymbol{\phi}}_0$ is a unit azimuthal vector, $I(\phi, z)$ is the surface density of the current, $\delta(\rho)$ is the Dirac function, and $|z| < d$. The unknown surface current density $I(\phi, z)$ also admits the representation

$$I(\phi, z) = \sum_{m=-\infty}^{\infty} \mathcal{I}_m(z) \exp(-jm\phi) \tag{7}$$

where the azimuthal harmonics $\mathcal{I}_m(z)$ of the antenna current are the desired functions of the coordinate z across the strip.

Since the antenna current is zero for $\rho < a$ and $\rho > a$, the electromagnetic fields in these regions are described by the source-free Maxwell equations. It can be shown from them that the longitudinal components of the electromagnetic field inside the cylinder satisfy the equations [27], [34], [35]

$$\nabla_\perp^2 E_z + \frac{\varepsilon_\parallel}{\varepsilon_\perp} \frac{\partial^2 E_z}{\partial z^2} + k_0^2 \varepsilon_\parallel \mu_\perp E_z = 0 \tag{8}$$

$$\nabla_\perp^2 H_z + \frac{\mu_\parallel}{\mu_\perp} \frac{\partial^2 H_z}{\partial z^2} + k_0^2 \varepsilon_\perp \mu_\parallel H_z = 0 \tag{9}$$

where $\nabla_\perp^2$ is the transverse (with respect to the z-axis) part of the Laplace operator and k_0 is the wavenumber in free space. It is evident that the field equations (8) and (9) correspond to the E and H waves, respectively. The other field components can be found from E_z and H_z.

Recall that the metamaterial is called hyperbolic if at least one of the following conditions is fulfilled for the elements of the tensors in (1) and (2):

$$\operatorname{sgn} \varepsilon_\perp \neq \operatorname{sgn} \varepsilon_\parallel \tag{10}$$

$$\operatorname{sgn} \mu_\perp \neq \operatorname{sgn} \mu_\parallel. \tag{11}$$

Then the refractive index surface of one of the normal waves, namely, of the E wave in the case (10) and the H wave in the case (11), has the shape of a one- or two-sheeted hyperboloid of revolution [4], [5]. If the inequalities in (10) and (11) are satisfied simultaneously, the refractive index surfaces of both normal waves have such a shape, and the metamaterial may be called doubly hyperbolic [27]. For the metamaterial with nonhyperbolic dispersion, the conditions

$$\operatorname{sgn} \varepsilon_\perp = \operatorname{sgn} \varepsilon_\parallel \tag{12}$$

$$\operatorname{sgn} \mu_\perp = \operatorname{sgn} \mu_\parallel \tag{13}$$

are satisfied simultaneously.

To obtain the field equations for an isotropic magnetodielectric medium outside the cylinder, one should make the replacements

$$\varepsilon_{\perp,\parallel} \to \varepsilon, \quad \mu_{\perp,\parallel} \to \mu \tag{14}$$

in (8) and (9).

The solutions of the field equations must be regular on the axis $\rho = 0$, satisfy the radiation condition at infinity, and ensure the fulfillment of the boundary conditions for the tangential field components on the cylinder surface $\rho = a$. In addition, the field should satisfy the boundary conditions

$$E_\phi + E_\phi^{ext} = 0 \tag{15}$$

$$E_z = 0 \tag{16}$$

on the antenna surface, i.e., at $\rho = a$ and $|z| < d$.

III. INTEGRAL EQUATIONS FOR THE ANTENNA CURRENT

To obtain a formal representation of the electromagnetic field due to the unknown current (7), we employ the Fourier transform technique. The longitudinal field components are related to their Fourier transforms by the integrals

$$\begin{bmatrix} E_z(\rho,\phi,z) \\ H_z(\rho,\phi,z) \end{bmatrix} = \sum_{m=-\infty}^{\infty} \frac{k_0}{2\pi} \int_{-\infty}^{\infty} \begin{bmatrix} E_{z;m}(\rho,p) \\ H_{z;m}(\rho,p) \end{bmatrix} \times \exp(-jm\phi - jk_0 pz)dp \tag{17}$$

where p is the longitudinal wavenumber normalized to k_0. Equations for the quantities $E_{z;m}(\rho, p)$ and $H_{z;m}(\rho, p)$ in the region $\rho < a$ are obtained from (8) and (9) as

$$\hat{L}_m E_{z;m} + k_0^2 \left(\varepsilon_\parallel \mu_\perp - \frac{\varepsilon_\parallel}{\varepsilon_\perp} p^2 \right) E_{z;m} = 0 \tag{18}$$

$$\hat{L}_m H_{z;m} + k_0^2 \left(\varepsilon_\perp \mu_\parallel - \frac{\mu_\parallel}{\mu_\perp} p^2 \right) H_{z;m} = 0 \tag{19}$$

where

$$\hat{L}_m = \frac{\partial^2}{\partial \rho^2} + \frac{1}{\rho}\frac{\partial}{\partial \rho} - \frac{m^2}{\rho^2}.$$

The Fourier transforms of the transverse field components are readily related to $E_{z;m}(\rho, p)$ and $H_{z;m}(\rho, p)$ by suitable differentiations [34], [35]. Performing the replacements (14), we can specialize (18) and (19) to the isotropic outer region of the cylinder ($\rho > a$).

Solving equations (18) and (19) and making use of some algebra, we can write the Fourier transforms of the field components as follows.

1) For $\rho < a$

$$E_{\rho;m}(\rho,p) = \frac{p}{\varepsilon_\perp} J_m'(k_0 q_1 \rho) A_m + m \frac{J_m(k_0 q_2 \rho)}{k_0 q_2 \rho} B_m$$

$$E_{\phi;m}(\rho,p) = -j \left[\frac{p}{\varepsilon_\perp} m \frac{J_m(k_0 q_1 \rho)}{k_0 q_1 \rho} A_m + J_m'(k_0 q_2 \rho) B_m \right]$$

$$E_{z;m}(\rho,p) = j \frac{q_1}{\varepsilon_\parallel} J_m(k_0 q_1 \rho) A_m$$

$$H_{\rho;m}(\rho,p) = jZ_0^{-1} \left[m \frac{J_m(k_0 q_1 \rho)}{k_0 q_1 \rho} A_m \right.$$

$$
\begin{aligned}
&\qquad + \frac{p}{\mu_\perp} J_m'(k_0 q_2 \rho) B_m \Big] \\
H_{\phi;m}(\rho,p) &= Z_0^{-1}\Big[J_m'(k_0 q_1 \rho) A_m \\
&\qquad + \frac{p}{\mu_\perp} m \frac{J_m(k_0 q_2 \rho)}{k_0 q_2 \rho} B_m \Big] \\
H_{z;m}(\rho,p) &= -Z_0^{-1} \frac{q_2}{\mu_\parallel} J_m(k_0 q_2 \rho) B_m. \qquad (20)
\end{aligned}
$$

2) For $\rho > a$

$$
\begin{aligned}
E_{\rho;m}(\rho,p) &= \frac{p}{\varepsilon} H_m^{(2)\prime}(k_0 q \rho) C_m + m \frac{H_m^{(2)}(k_0 q \rho)}{k_0 q \rho} D_m \\
E_{\phi;m}(\rho,p) &= -j\Big[\frac{p}{\varepsilon} m \frac{H_m^{(2)}(k_0 q \rho)}{k_0 q \rho} C_m \\
&\qquad + H_m^{(2)\prime}(k_0 q \rho) D_m \Big] \\
E_{z;m}(\rho,p) &= j \frac{q}{\varepsilon} H_m^{(2)}(k_0 q \rho) C_m \\
H_{\rho;m}(\rho,p) &= j Z_0^{-1}\Big[m \frac{H_m^{(2)}(k_0 q \rho)}{k_0 q \rho} C_m \\
&\qquad + \frac{p}{\mu} H_m^{(2)\prime}(k_0 q \rho) D_m \Big] \\
H_{\phi;m}(\rho,p) &= Z_0^{-1}\Big[H_m^{(2)\prime}(k_0 q \rho) C_m \\
&\qquad + \frac{p}{\mu} m \frac{H_m^{(2)}(k_0 q \rho)}{k_0 q \rho} D_m \Big] \\
H_{z;m}(\rho,p) &= -Z_0^{-1} \frac{q}{\mu} H_m^{(2)}(k_0 q \rho) D_m. \qquad (21)
\end{aligned}
$$

Hereafter, J_m and $H_m^{(l)}$ stand for the mth-order Bessel function of the first kind and Hankel function of the lth kind ($l = 1, 2$), respectively, J_m' and $H_m^{(l)\prime}$ are the derivatives of these functions with respect to the argument, $Z_0 = (\mu_0/\epsilon_0)^{1/2}$ is the impedance of free space, A_m, B_m, C_m, and D_m are constants to be determined, and

$$
\begin{aligned}
q_1 &= \left(\varepsilon_\parallel \mu_\perp - \frac{\varepsilon_\parallel}{\varepsilon_\perp} p^2\right)^{1/2}, \quad q_2 = \left(\varepsilon_\perp \mu_\parallel - \frac{\mu_\parallel}{\mu_\perp} p^2\right)^{1/2} \\
q &= (\varepsilon\mu - p^2)^{1/2}. \qquad (22)
\end{aligned}
$$

In the above, q_1 and q_2 are the normalized (to k_0) transverse wavenumbers of the E and H waves in a uniaxial metamaterial, respectively, and q is the analogous transverse wavenumber in the isotropic medium surrounding the metamaterial cylinder. The field components in (20) are regular on the z-axis, as required. To ensure the radiation condition at infinity for the solution comprising the second-kind Hankel functions in (21), the branch of q as a function of p in (22) must satisfy the inequality

$$
\operatorname{Im} q < 0. \qquad (23)
$$

If the imaginary part of q vanishes, one should introduce a minor loss in the surrounding medium when choosing the required branch according to (23) and then go over to the limiting case of a loss-free medium in the resultant expressions.

The coefficients A_m, B_m, C_m, and D_m are determined from the boundary conditions at the cylindrical interface $\rho = a$. According to the boundary conditions, the azimuthal field components and the longitudinal electric-field component are continuous at this interface, whereas the longitudinal magnetic-field component is continuous at $\rho = a$ for $|z| > d$ and undergoes a jump corresponding to the surface current (7) for $|z| < d$. Then

$$
H_{z;m}^{(-)} - H_{z;m}^{(+)} = \mathcal{I}_m(p). \qquad (24)
$$

Here, $H_{z;m}^{(-)}$ and $H_{z;m}^{(+)}$ denote the values of $H_{z;m}(\rho,p)$ on the inner ($\rho < a$) and outer ($\rho > a$) sides of the interface $\rho = a$, respectively. The quantity $\mathcal{I}_m(p)$, which determines the jump of $H_{z;m}(\rho,p)$ in (24), is the Fourier transform of $\mathcal{I}_m(z)$ with respect to the longitudinal coordinate, so that

$$
\mathcal{I}_m(p) = \int_{-d}^{d} \mathcal{I}_m(z') \exp(jk_0 p z') dz'. \qquad (25)
$$

When writing (25), use was made of the fact that the antenna current is zero for $|z| > d$. Hence, the function $\mathcal{I}_m(p)$ vanishes as its argument p tends to infinity. It can also be inferred from the symmetry of antenna excitation that $\mathcal{I}_m(z)$ and $\mathcal{I}_m(p)$ are even functions of their arguments.

Since the azimuthal and longitudinal components of the electric field, which will be needed in what follows, are continuous at the interface of two media, either the coefficients A_m and B_m or the coefficients C_m and D_m can be taken when deriving the expressions for these components on the surface $\rho = a$. We will employ the coefficients A_m and B_m, which are found to be

$$
\begin{aligned}
A_m &= -Z_0 k_0 a \frac{\varepsilon_\parallel}{\varepsilon} \frac{p}{Q^2} \frac{m \mathcal{I}_m(p) \tilde{A}_m^{(2)}}{Q_1 J_m(Q_1) \Delta_m^{(2)}} \\
B_m &= Z_0 k_0 a \mu_\parallel \frac{\mathcal{I}_m(p) \tilde{B}_m^{(2)}}{Q_2 J_m(Q_2) \Delta_m^{(2)}}. \qquad (26)
\end{aligned}
$$

Here and in what follows, we use the notations

$$
\begin{aligned}
\tilde{A}_m^{(l)} &= \Delta_{H,m}^{(l)} + \left(1 - \frac{\varepsilon_\parallel}{\varepsilon_\perp} \frac{Q^2}{Q_1^2}\right) \mathcal{H}_m^{(l)} \\
\tilde{B}_m^{(l)} &= \Delta_{E,m}^{(l)} \mathcal{H}_m^{(l)} + \frac{m^2}{\varepsilon\mu} \frac{p^2}{Q^4} \left(1 - \frac{\varepsilon_\parallel}{\varepsilon_\perp} \frac{Q^2}{Q_1^2}\right) \\
\Delta_m^{(l)} &= \Delta_{E,m}^{(l)} \Delta_{H,m}^{(l)} - \frac{m^2}{\varepsilon\mu} \frac{p^2}{Q^4} \left(1 - \frac{\varepsilon_\parallel}{\varepsilon_\perp} \frac{Q^2}{Q_1^2}\right)^2 \qquad (27)
\end{aligned}
$$

where

$$
\begin{aligned}
\Delta_{E,m}^{(l)} &= \frac{\varepsilon_\parallel}{\varepsilon} \mathcal{J}_m^{(1)} - \mathcal{H}_m^{(l)}, \quad \Delta_{H,m}^{(l)} = \frac{\mu_\parallel}{\mu} \mathcal{J}_m^{(2)} - \mathcal{H}_m^{(l)} \\
\mathcal{J}_m^{(l)} &= \frac{J_{m+1}(Q_l)}{Q_l J_m(Q_l)} - \frac{m}{Q_l^2}, \quad \mathcal{H}_m^{(l)} = \frac{H_{m+1}^{(l)}(Q)}{Q H_m^{(l)}(Q)} - \frac{m}{Q^2} \\
Q &= k_0 a q, \quad Q_l = k_0 a q_l, \quad l = 1, 2. \qquad (28)
\end{aligned}
$$

Substituting (26) into (20) and allowing for (25), we can write the azimuthal and longitudinal components of the antenna electric field at $\rho = a$ as

$$E_\phi(a, \phi, z) = \sum_{m=-\infty}^{\infty} \exp(-jm\phi) \int_{-d}^{d} K_m(z-z')\mathcal{I}_m(z')dz' \quad (29)$$

$$E_z(a, \phi, z) = \sum_{m=-\infty}^{\infty} \exp(-jm\phi) \int_{-d}^{d} k_m(z-z')\mathcal{I}_m(z')dz'. \quad (30)$$

In these representations, the kernels $K_m(\zeta)$ and $k_m(\zeta)$, with the argument $\zeta = z - z'$, are given by

$$K_m(\zeta) = jZ_0 \frac{k_0^2 a}{2\pi} \int_{-\infty}^{\infty} \frac{1}{\Delta_m^{(2)}} \left(\frac{m^2}{\varepsilon} \frac{\varepsilon_\parallel}{\varepsilon_\perp} \frac{p^2}{Q^2 Q_1^2} \tilde{A}_m^{(2)} + \mu_\parallel \mathcal{J}_m^{(2)} \tilde{B}_m^{(2)} \right) \exp(-jk_0 p\zeta)dp \quad (31)$$

$$k_m(\zeta) = -jZ_0 \frac{k_0}{2\pi\varepsilon} m \lim_{\rho \to a-0} \int_{-\infty}^{\infty} \frac{1}{\Delta_m^{(2)}} \frac{pJ_m(Q_1\rho/a)}{Q^2 J_m(Q_1)} \times \tilde{A}_m^{(2)} \exp(-jk_0 p\zeta)dp. \quad (32)$$

Since the solution obtained for the field in the inner region of the cylinder was used in deriving (31) and (32), the limiting transition $\rho \to a-0$ should be performed after evaluating the singular integral in (32). In (31), such a transition turns out to be possible under the integral sign without loss of accuracy.

Evaluation of the integrals in (31) and (32) is sufficiently simplified if the quantity q defined in (22) is chosen as a new integration variable and the integration path in the complex p plane is distorted so as to enclose all poles and branch singularities of the integrands. The integrands of (31) and (32) have the branch points $p = \pm(\varepsilon\mu)^{1/2}$, from which the corresponding branch cuts go along the lines $\operatorname{Im} q = 0$ in the complex p plane. In addition, these integrands may have poles at some points $p = p_{m,n}$ and $p = p_{m,-n} = -p_{m,n}$, where $\operatorname{Im} p_{m,n} < 0$. These poles are solutions of the equation

$$\Delta_m^{(2)} = 0 \quad (33)$$

and give the normalized propagation constants of the modes supported by the cylinder. In the above, n is the radial index of the mode ($n = 1, 2, \ldots$). The mode fields are also denoted by the subscripts m and n, and the functions $\mathbf{E}_{m,n}(\rho) = \mathbf{E}_m(\rho, p_{m,n})$ and $\mathbf{H}_{m,n}(\rho) = \mathbf{H}_m(\rho, p_{m,n})$, which describe the dependence of these fields on ρ, can be obtained from (20) and (21) by making the replacements of the coefficients A_m, B_m, C_m, and D_m with the coefficients $\mathcal{A}_{m,n}$, $\mathcal{B}_{m,n}$, $\mathcal{C}_{m,n}$, and $\mathcal{D}_{m,n}$, respectively. Expressions for the mode coefficients $\mathcal{A}_{m,n}$, $\mathcal{B}_{m,n}$, $\mathcal{C}_{m,n}$, and $\mathcal{D}_{m,n}$ can be found from the continuity condition for the tangential components of the mode fields at $\rho = a$. This leads to the requirement that the determinant of a system of homogeneous equations for the mode coefficients should be zero. It is this condition that is represented by (33). One of these coefficients may be chosen arbitrarily. To simplify relations between the fields of modes with the indices m and n and the indices $-m$ and $-n$, we put $\mathcal{A}_{m,n} = (-1)^m$ in rigorous expressions for these fields.

The location of the above-mentioned singularities is shown qualitatively in Fig. 2 in the case where $\varepsilon > 0$ and $\mu > 0$.

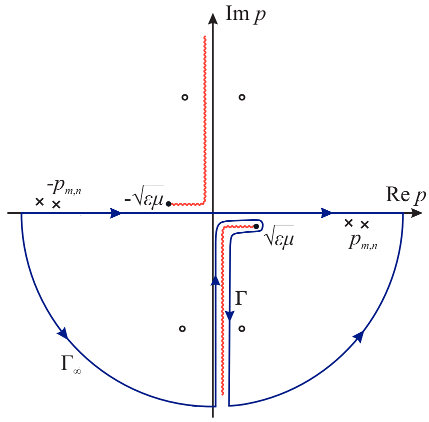

FIGURE 2. Singularities and paths of integration in the complex p plane for $\zeta > 0$. The black circles denote the branch points. The crosses and the light circles denote the location of the poles referring to propagating and complex modes, respectively.

Under these conditions, the branch cuts lie in the second and fourth quadrants of the p plane. The sheet of the complex p plane in Fig. 2 is specified by the inequality (23). Fig. 2 also depicts the distorted integration path enclosing the singularities located in the lower half of the complex p plane for $\zeta > 0$. Since the contribution of the semicircle Γ_∞ at infinity to the integrals in (31) and (32) is zero if $\zeta > 0$, they are determined by the sign-reversed residues at the poles $p = p_{m,n}$, which refer to the eigenmodes of the cylinder, and an integration around the branch cut, i.e., along the path Γ. In addition to the poles referring to the propagating modes, for which the quantities $p_{m,n}$ are purely real in the case of loss-free media, there may also be poles referring to complex modes. The complex modes always exist in pairs [36] such that if $p_{m,n}$ is a complex-valued solution of (33), then $-p_{m,n}^*$ is also a solution, provided the losses are absent. Here, the asterisk denotes complex conjugation. For $\zeta < 0$, the integration path should be distorted to go in the upper half of the p plane.

We note that the branch points, the branch cuts, and the poles corresponding to the propagating modes are slightly displaced off the axes in Fig. 2 due to a minor loss introduced to the outer region $\rho > a$. This makes it possible to clarify the mutual location of the integration paths and all the singularities of the integrands in the complex p plane. However, in the resulting expressions, the loss is put equal to zero. In the case $\varepsilon < 0$ and $\mu < 0$, the branch points and the branch cuts, in contrast to Fig. 2, lie in the first and third quadrants of the p plane. If $\varepsilon\mu < 0$, the branch points have purely imaginary values, and the branch cuts go from these points to infinity along the positive and negative imaginary semiaxes in the p plane. In all the above cases, it can be shown that $\operatorname{Re} q > 0$ in the first and third quadrants, whereas $\operatorname{Re} q < 0$ in the second and fourth quadrants of this plane.

In the above calculations, the quantity q runs all real values during the integration along Γ. Passing to integration over only the positive real q values allows one to represent the kernels (31) and (32) as the eigenfunction expansions [37]

$$K_m(\zeta) = jZ_0\frac{k_0^2 a}{2\pi}\sum_{l=1}^{2}\int_0^\infty \frac{(-1)^l}{\Delta_m^{(l)}}\left[\frac{m^2}{\varepsilon}\frac{\varepsilon_\parallel}{\varepsilon_\perp}\frac{p^2(q)}{Q^2Q_1^2}\tilde{A}_m^{(l)} + \mu_\parallel \mathcal{J}_m^{(2)}\tilde{B}_m^{(l)}\right]\frac{q}{p(q)}\exp[-jk_0p(q)|\zeta|]dq + \sum_n \frac{2\pi a}{N_{m,n}}E^2_{\phi;m,n}(a)\exp(-jk_0p_{m,n}|\zeta|) \quad (34)$$

$$k_m(\zeta) = \operatorname{sgn}\zeta\left[-jZ_0\frac{m}{2\pi k_0a^2\varepsilon}\sum_{l=1}^{2}\int_0^\infty \frac{(-1)^l}{q\Delta_m^{(l)}}\tilde{A}_m^{(l)} \times \exp[-jk_0p(q)|\zeta|]dq + \sum_n \frac{2\pi a}{N_{m,n}}E_{\phi;m,n}(a) \times E_{z;m,n}(a)\exp(-jk_0p_{m,n}|\zeta|)\right]. \quad (35)$$

The quantities entering the integrands of (34) and (35) are given by the same expressions as in (27) and (28) if one puts $p = p(q)$, where

$$p(q) = (\varepsilon\mu - q^2)^{1/2} \quad (36)$$

with $\operatorname{Im} p(q) < 0$, at least in the limit of vanishing losses. This means that the quantities q_1 and q_2, which are defined in (22), are now regarded as functions of q such that

$$q_1 = \left[\frac{\varepsilon_\parallel}{\varepsilon_\perp}(\varepsilon_\perp\mu_\perp - \varepsilon\mu + q^2)\right]^{1/2}$$
$$q_2 = \left[\frac{\mu_\parallel}{\mu_\perp}(\varepsilon_\perp\mu_\perp - \varepsilon\mu + q^2)\right]^{1/2}. \quad (37)$$

The quantity $N_{m,n}$ in (34) and (35) has the meaning of the norm of an eigenmode with the indices m and n and is given by the expression [29]

$$N_{m,n} = 4\pi\int_0^\infty \left[E_{\rho;m,n}(\rho)H_{\phi;m,n}(\rho) + E_{\phi;m,n}(\rho)H_{\rho;m,n}(\rho)\right]\rho\, d\rho. \quad (38)$$

In deriving the norm $N_{m,n}$ and the terms summed over n in (34) and (35), use was made of the fact that under the simultaneous replacements $m \to -m$ and $n \to -n$, the radial electric- and magnetic-field components of the modes reverse their signs, whereas the signs of the other components remain intact, provided that the coefficients $\mathcal{A}_{m,n}$, $\mathcal{B}_{m,n}$, $\mathcal{C}_{m,n}$, and $\mathcal{D}_{m,n}$ for the modes of the cylinder are introduced as described above. The proof that the contributions due to the poles at $p = p_{m,n}$ are reduced to the terms summed over n, as is indicated in (34) and (35), can be found in [37] and [38].

It is evident that the kernels (34) and (35) comprise the contributions due to the cylinder eigenmodes, i.e., the discrete-spectrum waves, and the contributions in the form of integrals over the continuous-spectrum waves, which correspond to the continuous spectrum of the positive real q values [36], [37], [38]. Such a spectral representation of the kernels turns out to be most convenient for the forthcoming analysis.

Using the boundary conditions (15) and (16) for the tangential components of the electric field on the antenna surface and bearing in mind formulas (4), (29), and (30), we can obtain integral equations for the quantities $\mathcal{I}_m(z)$. With allowance for the angular orthogonality of azimuthal harmonics, it follows from (15) that

$$\int_{-d}^{d} K_m(z - z')\mathcal{I}_m(z')dz' = -\mathcal{E}_m \quad (39)$$

whereas (16) gives

$$\int_{-d}^{d} k_m(z - z')\mathcal{I}_m(z')dz' = 0. \quad (40)$$

In integral equations (39) and (40), $m = 0, \pm 1, \pm 2, \ldots$ and $|z| < d$.

IV. ANALYSIS OF THE KERNELS OF THE INTEGRAL EQUATIONS

A. SINGULAR AND REGULAR PARTS OF THE KERNELS

The kernels (34) and (35) of integral equations (39) and (40) can be represented as the sums of singular and regular parts

$$K_m(\zeta) = K_m^{(s)}(\zeta) + K_m^{(r)}(\zeta)$$
$$k_m(\zeta) = k_m^{(s)}(\zeta) + k_m^{(r)}(\zeta). \quad (41)$$

The singular parts $K_m^{(s)}(\zeta)$ and $k_m^{(s)}(\zeta)$ comprise terms that tend to infinity for $\zeta \to 0$, whereas the regular parts $K_m^{(r)}(\zeta)$ and $k_m^{(r)}(\zeta)$ are finite in this limit. It turns out that in some cases, the singular parts of the kernels can be contributed by not only the continuous-spectrum waves but also the discrete-spectrum waves. Under such conditions, these quantities can be written as

$$K_m^{(s)}(\zeta) = K_m^{(s,\mathrm{cs})}(\zeta) + K_m^{(s,\mathrm{ds})}(\zeta)$$
$$k_m^{(s)}(\zeta) = k_m^{(s,\mathrm{cs})}(\zeta) + k_m^{(s,\mathrm{ds})}(\zeta) \quad (42)$$

where the additional superscripts "cs" and "ds" denote the contributions corresponding to the continuous- and discrete-spectrum waves, respectively. It is not difficult to verify that the singular quantities $K_m^{(s,\mathrm{cs})}(\zeta)$ and $k_m^{(s,\mathrm{cs})}(\zeta)$ are yielded by taking the limit $q \to \infty$ in the integrands of (34) and (35), respectively. In this limit, the following relations take place:

$$p(q) = -jq, \quad q_1^2 = (\varepsilon_\parallel/\varepsilon_\perp)q^2, \quad q_2^2 = (\mu_\parallel/\mu_\perp)q^2$$
$$\Delta_m^{(l)} = \Delta_{E,m}^{(l)}\Delta_{H,m}^{(l)}, \quad \tilde{A}_m^{(l)} = \Delta_{H,m}^{(l)}, \quad \tilde{B}_m^{(l)} = \Delta_{E,m}^{(l)}\mathcal{H}_m^{(l)}. \quad (43)$$

Making use of (43), one obtains

$$K_m^{(s,\mathrm{cs})}(\zeta) = Z_0\frac{k_0^2a}{2\pi}\sum_{l=1}^{2}\int_0^\infty (-1)^l\left[\frac{m^2}{(k_0a)^4\varepsilon}\frac{1}{q^2\Delta_{E,m}^{(l)}} - \mu_\parallel\frac{\mathcal{J}_m^{(2)}\mathcal{H}_m^{(l)}}{\Delta_{H,m}^{(l)}}\right]\exp(-k_0|\zeta|q)dq \quad (44)$$

$$k_m^{(s,\mathrm{cs})}(\zeta) = -jZ_0\frac{m\operatorname{sgn}\zeta}{2\pi k_0a^2\varepsilon}\sum_{l=1}^{2}\int_0^\infty \frac{(-1)^l}{q\Delta_{E,m}^{(l)}} \times \exp(-k_0|\zeta|q)dq. \quad (45)$$

It is seen that the integrand of (44) is determined by the additive terms corresponding to the E and H waves of the metamaterial, whereas the integrand of (45), by only the E-wave term.

The singular terms $K_m^{(s,\mathrm{ds})}(\zeta)$ and $k_m^{(s,\mathrm{ds})}(\zeta)$ appear only if the metamaterial cylinder is capable of supporting an infinite set of eigenmodes with the propagation constants satisfying the condition $|p_{m,n}| \to \infty$ at $n \to \infty$. Then the quantities $K_m^{(s,\mathrm{ds})}(\zeta)$ and $k_m^{(s,\mathrm{ds})}(\zeta)$ are given by infinite series whose terms are contributions of the eigenmodes, i.e., the discrete-spectrum waves, which are taken in the limit $|p_{m,n}| \to \infty$. Otherwise the discrete-spectrum waves do not contribute to the singular parts of the kernels.

The regular parts of the kernels are also determined by the contributions related to the continuous- and discrete-spectrum waves. The contributions of the continuous-spectrum waves to $K_m^{(r)}(\zeta)$ and $k_m^{(r)}(\zeta)$ are obtained by replacing the integrands in (34) and (35) with the differences of the respective integrands and their limits at $q \to \infty$. Similarly, the contributions of the discrete-spectrum waves to $K_m^{(r)}(\zeta)$ and $k_m^{(r)}(\zeta)$ are yielded by replacing the terms summed over n in (34) and (35) with the differences of these terms and their limits at $|p_{m,n}| \to \infty$. Clearly, the latter procedure is required only if the terms $K_m^{(s,\mathrm{ds})}(\zeta)$ and $k_m^{(s,\mathrm{ds})}(\zeta)$ arise in the analysis. We will not present here cumbersome expressions for $K_m^{(r)}(\zeta)$ and $k_m^{(r)}(\zeta)$, which can be evaluated only numerically, and focus on obtaining closed-form results for the singular parts of the kernels. With such results, integral equations (39) and (40) can be solved analytically if the strip conductor is sufficiently narrow such that

$$d \ll a\gamma_1, \quad d \ll a\gamma_2$$
$$(k_0 d)^2 \max\{|\varepsilon_{\perp,\parallel}|, |\mu_{\perp,\parallel}|, |\varepsilon|, |\mu|\} \ll 1 \tag{46}$$

where $\gamma_1 = |\varepsilon_\parallel/\varepsilon_\perp|^{1/2}$ and $\gamma_2 = |\mu_\parallel/\mu_\perp|^{1/2}$.

In what follows, the singular parts of the kernels will be analyzed separately in the cases where both normal waves of the metamaterial simultaneously have hyperbolic or nonhyperbolic dispersion, or where these waves are characterized by different types of dispersion.

B. DOUBLY HYPERBOLIC METAMATERIAL

In the case of a doubly hyperbolic metamaterial, where the inequalities (10) and (11) are satisfied simultaneously, both normal waves of the metamaterial in the cylinder have hyperbolic dispersion. In this case, it is convenient to introduce the following notations:

$$\varepsilon_u = -j|\varepsilon_\perp\varepsilon_\parallel|^{1/2}, \quad \mu_u = -j|\mu_\perp\mu_\parallel|^{1/2}. \tag{47}$$

Then, making use of the fact that $q_{1,2} = j\gamma_{1,2}q$ at $q \to \infty$ for such a metamaterial and taking (43) into account, we can replace the cylindrical functions in (43)–(45) by the large-argument approximations. For $K_m^{(s,\mathrm{cs})}(\zeta)$, this yields

$$K_m^{(s,\mathrm{cs})}(\zeta) = j\frac{Z_0}{\pi k_0 a^2}\left[m^2\frac{\varepsilon}{|\varepsilon_u|^2}\tilde{I}_m^{(1)} - (k_0 a)^2\mu\tilde{I}_m^{(2)}\right] \tag{48}$$

where the first and second terms correspond to the respective terms in the integrand of (44) and are written as

$$\tilde{I}_m^{(1)} = \int_0^\infty \frac{I_m^2(k_0 a\gamma_1 q)\exp(-k_0|\zeta|q)}{q[I_{m+1}^2(k_0 a\gamma_1 q) + \alpha_1^2 I_m^2(k_0 a\gamma_1 q)]}dq \tag{49}$$

$$\tilde{I}_m^{(2)} = \int_0^\infty \frac{I_{m+1}^2(k_0 a\gamma_2 q)\exp(-k_0|\zeta|q)}{q[I_{m+1}^2(k_0 a\gamma_2 q) + \alpha_2^2 I_m^2(k_0 a\gamma_2 q)]}dq. \tag{50}$$

Hereafter, $\alpha_1 = |\varepsilon/\varepsilon_u|$, $\alpha_2 = |\mu/\mu_u|$, and I_m is the modified Bessel function of the first kind of order m. Note that the integral in (49) is considered only for $m \neq 0$ in view of the fact that the first term in the brackets of (48) is zero for $m = 0$. Since (49) and (50) were derived in the limit $q \to \infty$, we can equate I_{m+1} to I_m in the numerator of (50) and replace the denominators of (49) and (50) by the large-argument approximations. Then we arrive at the table integral [39]

$$\begin{aligned}\tilde{I}_m^{(1,2)} &= \frac{2\pi k_0 a\gamma_{1,2}}{1+\alpha_{1,2}^2}\int_0^\infty I_{|m|}^2(k_0 a\gamma_{1,2}q) \\ &\quad\times \exp[-k_0(2a\gamma_{1,2} + |\zeta|)q]dq \\ &= \frac{2}{1+\alpha_{1,2}^2}Q_{|m|-\frac{1}{2}}\left(1 + \frac{2|\zeta|}{a\gamma_{1,2}} + \frac{\zeta^2}{2a^2\gamma_{1,2}^2}\right)\end{aligned} \tag{51}$$

where $Q_\nu(z)$ is the Legendre function of the second kind. By virtue of the first two inequalities in (46), the argument of the Legendre function in (51) differs only slightly from unity. In this case, the Legendre function can be approximated using the logarithmic function of ζ [40]. As a result, with allowance for (47), the quantity (48) reduces to

$$\begin{aligned}K_m^{(s,\mathrm{cs})}(\zeta) = -j\frac{Z_0}{\pi k_0 a^2}\Bigg\{&\left[\frac{m^2\varepsilon}{\varepsilon^2-\varepsilon_u^2} + \frac{(k_0 a)^2\mu\mu_u^2}{\mu^2-\mu_u^2}\right]\ln\frac{|\zeta|}{2a} \\ &+ \frac{m^2\varepsilon}{\varepsilon^2-\varepsilon_u^2}r_m^{(1)} + \frac{(k_0 a)^2\mu\mu_u^2}{\mu^2-\mu_u^2}r_m^{(2)}\Bigg\}\end{aligned} \tag{52}$$

where

$$r_m^{(1,2)} = 2\gamma + \ln(2/\gamma_{1,2}) + 2\psi\left(|m| + 1/2\right). \tag{53}$$

Here, $\gamma = 0.5772\ldots$ is Euler's constant and $\psi(z) = d\ln\Gamma(z)/dz$ is the logarithmic derivative of the gamma function $\Gamma(z)$. Note that the asymptotic representation for the Legendre function, which was used to obtain (52) and (53), needs to be corrected for very large values of $|m|$. However, under the condition $M = [\Delta^{-1}] \gg 1$, where the square brackets denote the integer part of the number, most contributions to the surface current density (7) of the antenna come from the terms with $|m| < M$ because of the properties of quantities (5) that will enter the resulting expression for $\mathcal{I}_m$. It can be shown that the requirement for formulas (52) and (53) to be valid for approximating the quantities $K_m^{(s,\mathrm{cs})}(\zeta)$ for $|m| < M$ reduces to the conditions

$$d \ll 2a\gamma_1\Delta, \quad d \ll 2a\gamma_2\Delta \tag{54}$$

which are assumed to be fulfilled.

The contribution of the discrete-spectrum waves to the singular part of the considered kernel is written as

$$K_m^{(s,\mathrm{ds})}(\zeta)=-j\frac{2Z_0}{\pi k_0 a^2}\left[\frac{m^2\varepsilon_u}{\varepsilon^2-\varepsilon_u^2}\tilde{S}_m^{(1)}+\frac{(k_0a)^2\mu^2\mu_u}{\mu^2-\mu_u^2}\tilde{S}_m^{(2)}\right] \quad (55)$$

where

$$\tilde{S}_m^{(1,2)}=\sum_{n=1}^{\infty}\frac{\exp[-j\sigma_{1,2}\chi_{1,2}(2n+|m|+1/2)]}{2n+|m|+1/2}. \quad (56)$$

Here, $\sigma_1=\operatorname{sgn}\varepsilon_\perp$, $\sigma_2=\operatorname{sgn}\mu_\perp$, and $\chi_{1,2}=\pi|\zeta|/(2a\gamma_{1,2})$. The derivation of (55) and (56) is given in Appendix A.

The conditions (54) enable us to rewrite the series (56) as

$$\tilde{S}_m^{(1,2)}=\sum_{n=1}^{\infty}\frac{\exp\left[-j\sigma_{1,2}\chi_{1,2}(2n-1)\right]}{2n-1}-\Phi_m \quad (57)$$

where

$$\Phi_m=(|m|+3/2)\sum_{n=1}^{\infty}\frac{1}{(2n-1)(2n+|m|+1/2)}. \quad (58)$$

When writing (58), we put $\zeta=0$ since the series yielding Φ_m is convergent for $\zeta\to 0$. The series in (57) can be represented in closed form [41]:

$$\sum_{n=1}^{\infty}\frac{\exp[-j\sigma_{1,2}\chi_{1,2}(2n-1)]}{2n-1}=\frac{1}{2}\ln\cot\frac{\chi_{1,2}}{2}-j\frac{\pi\sigma_{1,2}}{4}. \quad (59)$$

Making use of the fact that $\cot(\chi_{1,2}/2)\to 2\chi_{1,2}^{-1}$ at $\zeta\to 0$, we find

$$\tilde{S}_m^{(1,2)}=-\frac{1}{2}\left[\ln\frac{|\zeta|}{2a}+s_m^{(1,2)}\right] \quad (60)$$

where

$$s_m^{(1,2)}=\ln\frac{\pi}{2\gamma_{1,2}}+2\Phi_m+j\frac{\pi\sigma_{1,2}}{2}. \quad (61)$$

Finally, allowing for (52) and substituting (60) into (55), we obtain

$$K_m(\zeta)=-jZ_0\frac{k_0}{2\pi\beta_m}\ln\frac{|\zeta|}{2a}+K_{\Sigma,m}^{(r)} \quad (62)$$

so that the integral equation (39) takes the form

$$\int_{-d}^{d}\mathcal{I}_m(z')\ln\frac{|z-z'|}{2a}dz' =-j\frac{2\pi\beta_m}{Z_0k_0}\left[\mathcal{E}_m+K_{\Sigma,m}^{(r)}\int_{-d}^{d}\mathcal{I}_m(z')dz'\right]. \quad (63)$$

Here,

$$\beta_m=\frac{(k_0a)^2\varepsilon_{\mathrm{eff}}}{m^2-(k_0a)^2\varepsilon_{\mathrm{eff}}\mu_{\mathrm{eff}}} \quad (64)$$

where the quantities $\varepsilon_{\mathrm{eff}}$ and μ_{eff} are defined by the relations

$$\varepsilon_{\mathrm{eff}}=\frac{\varepsilon+\varepsilon_u}{2},\quad \mu_{\mathrm{eff}}=\frac{2\mu\mu_u}{\mu+\mu_u} \quad (65)$$

and $K_{\Sigma,m}^{(r)}$ is the total regular part, which comprises all partial regular parts of $K_m(\zeta)$, including those that appeared during the derivation of (52) and (60). Then, the quantity $K_{\Sigma,m}^{(r)}$ in (63) is written as

$$K_{\Sigma,m}^{(r)}=K_m^{(r)}(0)-j\frac{Z_0k_0}{\pi}\left[\frac{m^2(\varepsilon r_m^{(1)}-\varepsilon_u s_m^{(1)})}{(k_0a)^2(\varepsilon^2-\varepsilon_u^2)}+\frac{\mu\mu_u(\mu_u r_m^{(2)}-\mu s_m^{(2)})}{\mu^2-\mu_u^2}\right] \quad (66)$$

where we put $\zeta=0$ in the regular term $K_m^{(r)}(\zeta)$, which is possible by virtue of the last inequality in (46).

In turn, the quantity $k_m^{(s)}(\zeta)$, with application of (45), is reduced to the form

$$k_m^{(s)}(\zeta)=\operatorname{sgn}\zeta\,\frac{Z_0}{k_0a^2}\frac{m}{\varepsilon^2-\varepsilon_u^2}\times\left\{\frac{k_0a\varepsilon}{\pi}\int_0^\infty\exp(-k_0|\zeta|q)dq-\varepsilon_\perp\lim_{\nu\to 0}\sum_{n=1}^{\infty}\exp\left[-\chi_1(j\sigma_1+\nu)\times(2n+|m|+1/2)\right]\right\}. \quad (67)$$

The details of the derivation of the sum in (67) are discussed in Appendix A. Making use of the first inequality in (54), we can neglect $|m|+1/2$ in (67). Then, for $\zeta\to 0$, one obtains

$$k_m^{(s)}(\zeta)=Z_0\frac{m}{2\pi k_0a\varepsilon_{\mathrm{eff}}}\frac{1}{\zeta}. \quad (68)$$

Allowing for (68) and replacing the regular part of $k_m(\zeta)$ by $k_m^{(r)}(0)$, which is found to be zero through careful examination, one has from (40) that

$$\int_{-d}^{d}m\frac{\mathcal{I}_m(z')}{z-z'}dz'=0 \quad (69)$$

where the integral is taken in the sense of the Cauchy principal value.

Thus, it is seen that the problem reduces to solving integral equations (63) and (69) for $\mathcal{I}_m(z)$. As is known from the theory of singular integral equations [42], the exact solution of the equation (63) with a logarithmic kernel automatically satisfies the equation (69) with Cauchy's kernel. This enables us to consider only the integral equation (63) in what follows.

C. NONHYPERBOLIC METAMATERIAL

We now proceed to the case of a nonhyperbolic metamaterial, for which conditions (12) and (13) are satisfied simultaneously. In this case, instead of (47), we will use the following notations:

$$\varepsilon_u=(\varepsilon_\perp\varepsilon_\parallel)^{1/2}\sigma_1,\quad \mu_u=(\mu_\perp\mu_\parallel)^{1/2}\sigma_2. \quad (70)$$

For both normal waves with nonhyperbolic dispersion in the metamaterial, one has $q_{1,2}=\gamma_{1,2}q$ at $q\to\infty$. In this limit, the quantity $K_m^{(s,\mathrm{cs})}(\zeta)$ coincides in form with (48), where the integrals $\tilde{I}_m^{(1)}$ and $\tilde{I}_m^{(2)}$ should be taken as

$$\tilde{I}_m^{(1)}=\int_0^\infty\frac{J_m^2(k_0a\gamma_1q)\exp(-k_0|\zeta|q)}{q[J_{m+1}^2(k_0a\gamma_1q)+\alpha_1^2J_m^2(k_0a\gamma_1q)]}dq \quad (71)$$

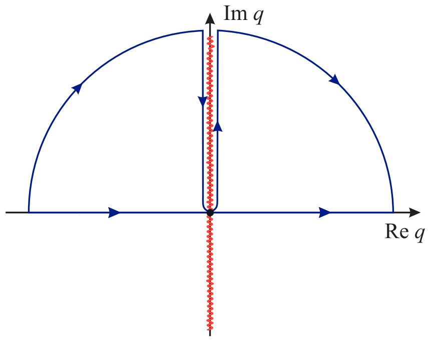

FIGURE 3. Singularities and paths of integration in the complex q plane showing the sheet in which $\mathrm{Im}\,\tilde{p}(q) < 0$. In this sheet, $\mathrm{Re}\,\tilde{p}(q) > 0$ in the first and third quadrants, and $\mathrm{Re}\,\tilde{p}(q) < 0$ in the second and fourth quadrants.

$$\tilde{I}_m^{(2)} = \int_0^\infty \frac{J_{m+1}^2(k_0 a\gamma_2 q)\exp(-k_0|\zeta|q)}{q[J_{m+1}^2(k_0 a\gamma_2 q) + \alpha_2^2 J_m^2(k_0 a\gamma_2 q)]}dq. \quad (72)$$

Here, α_1 and α_2 have the same meaning as in (49) and (50).

Integrals (71) and (72) are readily evaluated and reduced to the Legendre functions of the second kind if $\alpha_{1,2} = 1$ [39]. For $\alpha_{1,2} \neq 1$, a more involved procedure is required to evaluate these integrals. To do this, we introduce an auxiliary function $\tilde{p}(q) = (-q^2)^{1/2}$ and choose its branch so as to ensure the condition $\mathrm{Im}\,\tilde{p}(q) < 0$. This function has a branch point $q = 0$ and two branch cuts going from this point along the positive and negative imaginary semiaxes in the complex q plane, as is shown in Fig. 3. Performing analytic continuation of the integrands of (71) and (72) to the complex q plane, one can transform the corresponding integrals as

$$\tilde{I}_m^{(1)} = \frac{1}{2\alpha_1}\int_{-\infty}^{\infty}\frac{1}{\tilde{p}(q)}\left[\frac{J_{m+1}(k_0 a\gamma_1 q)}{J_m(k_0 a\gamma_1 q)} + j\alpha_1\right]^{-1} \times \exp[-jk_0|\zeta|\tilde{p}(q)]dq \quad (73)$$

$$\tilde{I}_m^{(2)} = \frac{1}{2j}\int_{-\infty}^{\infty}\frac{1}{\tilde{p}(q)}\left[\frac{J_{m+1}(k_0 a\gamma_2 q)}{J_m(k_0 a\gamma_2 q)} + j\alpha_2\right]^{-1} \times \frac{J_{m+1}(k_0 a\gamma_2 q)}{J_m(k_0 a\gamma_2 q)}\exp[-jk_0|\zeta|\tilde{p}(q)]dq. \quad (74)$$

The integrands of (73) and (74) have poles in the lower half of the complex q plane but do not have them in the upper half. Therefore, it is convenient to deform the integration path to a semicircle at infinity in the upper half-plane. Since this semicircle does not contribute anything to the integrals, there will be a contribution due only to an integration around the branch cut going along the positive imaginary semiaxis in the q plane. Passing to the new integration variable $\tilde{p}$, which takes purely real values on the sides of this branch cut, and then to integration over the positive values of $\tilde{p}$, one obtains

$$\tilde{I}_m^{(1)} = \frac{1}{\alpha_1}\int_0^\infty \frac{I_m(k_0 a\gamma_1\tilde{p})\cos(k_0\zeta\tilde{p})}{\tilde{p}[I_{m+1}(k_0 a\gamma_1\tilde{p}) + \alpha_1 I_m(k_0 a\gamma_1\tilde{p})]}d\tilde{p} \quad (75)$$

$$\tilde{I}_m^{(2)} = \int_0^\infty \frac{I_{m+1}(k_0 a\gamma_2\tilde{p})\cos(k_0\zeta\tilde{p})}{\tilde{p}[I_{m+1}(k_0 a\gamma_2\tilde{p}) + \alpha_2 I_m(k_0 a\gamma_2\tilde{p})]}d\tilde{p}. \quad (76)$$

It is shown in Appendix B that these integrals are reduced to

$$\tilde{I}_m^{(1)} = -\frac{1}{\alpha_1(1+\alpha_1)}\left(\ln\frac{|\zeta|}{2a} + r_m^{(1)}\right) + \delta\tilde{I}_m^{(1)} \quad (77)$$

$$\tilde{I}_m^{(2)} = -\frac{1}{1+\alpha_2}\left(\ln\frac{|\zeta|}{2a} + r_m^{(2)}\right) + \delta\tilde{I}_m^{(2)} \quad (78)$$

where $r_m^{(1)}$ and $r_m^{(2)}$ are defined by (53), and $\delta\tilde{I}_m^{(1)}$ and $\delta\tilde{I}_m^{(2)}$ are regular terms introduced in formulas (111) and (112) of Appendix B. Bearing in mind that, according to (48), $\tilde{I}_m^{(1)}$ and $\tilde{I}_m^{(2)}$ are multiplied by $\varepsilon/|\varepsilon_u|^2$ and μ, respectively, during the derivation of $K_m^{(s,\mathrm{cs})}(\zeta)$, we will employ the relations

$$\frac{\varepsilon}{|\varepsilon_u|^2}\frac{1}{\alpha_1(1+\alpha_1)} = \begin{cases} \dfrac{1}{\varepsilon+\varepsilon_u} & \text{for } \mathrm{sgn}\,\varepsilon = \mathrm{sgn}\,\varepsilon_u \\ \dfrac{1}{\varepsilon-\varepsilon_u} & \text{for } \mathrm{sgn}\,\varepsilon \neq \mathrm{sgn}\,\varepsilon_u \end{cases} \quad (79)$$

$$\frac{\mu}{1+\alpha_2} = \begin{cases} \dfrac{\mu\mu_u}{\mu+\mu_u} & \text{for } \mathrm{sgn}\,\mu = \mathrm{sgn}\,\mu_u \\ \dfrac{\mu\mu_u}{\mu_u-\mu} & \text{for } \mathrm{sgn}\,\mu \neq \mathrm{sgn}\,\mu_u. \end{cases} \quad (80)$$

A close examination shows that the discrete-spectrum waves do not contribute to the singular parts of the kernels of the integral equations for the antenna current if the conditions $\mathrm{sgn}\,\varepsilon = \mathrm{sgn}\,\varepsilon_u$ and $\mathrm{sgn}\,\mu = \mathrm{sgn}\,\mu_u$ are satisfied simultaneously. In this case, substituting (77) and (78) into (48), with allowance for (79) and (80), yields the previously obtained integral equation (63) with the already introduced notations (64) and (65). But now the quantities ε_u and μ_u are defined by expressions (70), and the total regular part $K_{\Sigma,m}^{(r)}$ should be calculated anew for each m. Hereafter, we will not write down the cumbersome expressions for $K_{\Sigma,m}^{(r)}$ since they can readily be obtained from the derivations described above.

If the conditions $\mathrm{sgn}\,\varepsilon = \mathrm{sgn}\,\varepsilon_u$ and $\mathrm{sgn}\,\mu = \mathrm{sgn}\,\mu_u$, or either of them, are not satisfied, the complex eigenmodes of a cylindrical nonhyperbolic metamaterial turn out to exist and contribute to the singular parts of the kernels. The contribution of such discrete-spectrum waves is again described by (55), where $\tilde{S}_m^{(1)} \neq 0$ if $\mathrm{sgn}\,\varepsilon \neq \mathrm{sgn}\,\varepsilon_u$, and $\tilde{S}_m^{(2)} \neq 0$ if $\mathrm{sgn}\,\mu \neq \mathrm{sgn}\,\mu_u$. For nonzero $\tilde{S}_m^{(1,2)}$, instead of (56), we now have

$$\tilde{S}_m^{(1,2)} = \sum_{n=1}^{\infty}\sum_{k=1}^{2}\frac{\exp[-\chi_{1,2}(2n+|m|+1/2)]}{2n+|m|+1/2+j2\pi^{-1}\xi_k^{(1,2)}}. \quad (81)$$

Here, $\chi_{1,2}$ has the same meaning as in (56) and

$$\xi_k^{(1,2)} = \begin{cases}(-1)^k\,\mathrm{artanh}\,\alpha_{1,2} & \text{for } \alpha_{1,2} < 1 \\ (-1)^k\,\mathrm{artanh}\,\alpha_{1,2}^{-1} - j\pi/2 & \text{for } \alpha_{1,2} > 1\end{cases} \quad (82)$$

where $k = 1, 2$. Expression (81), the derivation of which is discussed in Appendix C, is valid under the conditions

$$d|\xi_k^{(1)}| \ll a\gamma_1, \quad d|\xi_k^{(2)}| \ll a\gamma_2. \quad (83)$$

Assuming again the fulfillment of (54), one can rewrite (81) by analogy with (57) as

$$\tilde{S}_m^{(1,2)} = \sum_{n=1}^{\infty} \frac{\exp(-2\chi_{1,2}n)}{n} - \Psi_m^{(1,2)} \quad (84)$$

where

$$\Psi_m^{(1,2)} = \sum_{n=1}^{\infty}\sum_{k=1}^{2} \frac{|m| + 1/2 + j2\pi^{-1}\xi_k^{(1,2)}}{2n(2n + |m| + 1/2 + j2\pi^{-1}\xi_k^{(1,2)})}. \quad (85)$$

The series in (84) is found to be [41]

$$\sum_{n=1}^{\infty} \frac{\exp(-2\chi_{1,2}n)}{n} = -\ln[1 - \exp(-2\chi_{1,2})]. \quad (86)$$

Making use of the fact that $1 - \exp(-2\chi_{1,2}) \to 2\chi_{1,2}$ at $\zeta \to 0$, we find

$$\tilde{S}_m^{(1,2)} = -\ln\frac{|\zeta|}{2a} - \ln\frac{2\pi}{\gamma_{1,2}} - \Psi_m^{(1,2)}. \quad (87)$$

Combining (48), (55), (77)–(80), and (87) in the case where the complex modes contribute to the singular part of the kernel $K_m(\zeta)$, we again arrive at (63)–(65) with an appropriately calculated regular term $K_{\Sigma,m}^{(r)}$ and the quantities ε_u and μ_u, which are given by (70). The corresponding analysis for the kernel $k_m(\zeta)$ yields the previously obtained integral equation (69).

To avoid misunderstanding, it should be noted that the above analysis, performed for (81) in the case of a nonhyperbolic metamaterial cylinder, ceases to be valid if $\varepsilon_u \to -\varepsilon$ or $\mu_u \to -\mu$. Then $\alpha_1 \to 1$ or $\alpha_2 \to 1$, which results in violation of (83). However, it will be demonstrated below that such a situation, when $\varepsilon_{\text{eff}} \to 0$ or $\mu_{\text{eff}} \to \infty$, is of little interest to antenna applications and, therefore, need not be considered.

D. SINGLY HYPERBOLIC METAMATERIAL

By "singly" hyperbolic metamaterial, we mean a metamaterial in which only one normal wave has hyperbolic dispersion, while the other is characterized by the usual nonhyperbolic dispersion. Clearly, in this case the analysis is reduced to combining the results of the preceding sections.

Thus, under the conditions (10) and (13), the E-wave contribution to the kernels of the integral equations is considered as that for a doubly hyperbolic metamaterial, whereas the H-wave contribution, as that for a nonhyperbolic metamaterial. This leads to the integral equations derived above with the quantity ε_u given in (47) and the quantity μ_u given in (70). On the contrary, under the conditions (11) and (12), the E-wave contribution to the kernels of the integral equations is considered as that for a nonhyperbolic metamaterial, whereas the H-wave contribution, as that for a doubly hyperbolic metamaterial. Then the integral equations will contain the quantity ε_u given in (70) and the quantity μ_u given in (47).

The regular terms $K_{\Sigma,m}^{(r)}$ for different indices m should be calculated individually in each of the abovementioned special cases.

V. CURRENT DISTRIBUTION AND INPUT IMPEDANCE OF A LOOP ANTENNA

A. DERIVATION OF THE CURRENT DISTRIBUTION AND THE INPUT IMPEDANCE

It follows from the analysis performed that determining the current distribution of the considered antenna reduces to solving the integral equation

$$\int_{-d}^{d} \mathcal{I}_m(z')\ln\frac{|z-z'|}{2a}dz' = -j\frac{2\pi\beta_m}{Z_0k_0}\mathcal{E}_m - S_m\int_{-d}^{d}\mathcal{I}_m(z')dz' \quad (88)$$

where

$$S_m = j2\pi\beta_m(Z_0k_0)^{-1}K_{\Sigma,m}^{(r)}. \quad (89)$$

In all the special cases discussed above, the factor β_m is determined by the expression (64), which contains the effective parameters ε_{eff} and μ_{eff} defined by (65). Summarizing the results of the preceding sections, we can write the quantities ε_u and μ_u, which enter the parameters (65), as follows:

$$\varepsilon_u = \begin{cases} -j|\varepsilon_\perp\varepsilon_\parallel|^{1/2} & \text{for } \operatorname{sgn}\varepsilon_\perp \neq \operatorname{sgn}\varepsilon_\parallel \\ (\varepsilon_\perp\varepsilon_\parallel)^{1/2}\operatorname{sgn}\varepsilon_\perp & \text{for } \operatorname{sgn}\varepsilon_\perp = \operatorname{sgn}\varepsilon_\parallel \end{cases} \quad (90)$$

$$\mu_u = \begin{cases} -j|\mu_\perp\mu_\parallel|^{1/2} & \text{for } \operatorname{sgn}\mu_\perp \neq \operatorname{sgn}\mu_\parallel \\ (\mu_\perp\mu_\parallel)^{1/2}\operatorname{sgn}\mu_\perp & \text{for } \operatorname{sgn}\mu_\perp = \operatorname{sgn}\mu_\parallel. \end{cases} \quad (91)$$

The exact solution of the integral equation (88) can be obtained as described in [42] and has the form

$$\mathcal{I}_m(z) = \frac{2j}{Z_0k_0\sqrt{d^2-z^2}}\frac{\beta_m\mathcal{E}_m}{\ln(4a/d) - S_m}. \quad (92)$$

The total current $I_\Sigma(\phi)$ in the cross section $\phi = \text{const}$ of the antenna conductor is obtained by substituting (92) into (7) and integrating the quantity $I(\phi, z)$ over z between $-d$ and d:

$$I_\Sigma(\phi) = \int_{-d}^{d} I(\phi,z)dz = j\frac{V_0}{Z_0k_0a}\sum_{m=-\infty}^{\infty}\frac{\sin(m\Delta)}{m\Delta} \times \frac{\beta_m\exp[-jm(\phi-\phi_0)]}{\ln(4a/d) - S_m}. \quad (93)$$

Note that the total current (93) is finite despite the divergent behavior of (92) at $|z| \to d$, which corresponds to the Meixner edge condition [43]. The representation (93) is somewhat simplified by making use of the fact that $\beta_m = \beta_{-m}$ and $S_m = S_{-m}$. This gives

$$I_\Sigma(\phi) = j\frac{V_0}{Z_0k_0a}\sum_{m=0}^{\infty}(2-\delta_{m,0})\frac{\sin(m\Delta)}{m\Delta} \times \frac{\beta_m\cos[m(\phi-\phi_0)]}{\ln(4a/d) - S_m} \quad (94)$$

where $\delta_{m,n}$ is the Kronecker delta.

In the case of a rather narrow strip where $\ln(4a/d) \gg |S_m|$ for $0 \le m \le M$, one can neglect the terms S_m, put $\sin(m\Delta)/(m\Delta) \simeq 1$ for such m, and proceed to the summation over m from 0 to M in the series of (94). Since $M \gg 1$, the summation of the approximated terms of this series can be extended to all values of m from 0 to ∞. The resulting series is summable [41] and reduces to

$$I_\Sigma(\phi) = -j\frac{V_0\pi k_0\varepsilon_{\rm eff}}{Z_0 h\ln(4a/d)}\frac{\cos[(\pi+\phi_0-\phi)ha]}{\sin(\pi ha)} \quad (95)$$

where $h = k_0(\varepsilon_{\rm eff}\mu_{\rm eff})^{1/2}$, $ha \neq m$, and $0 \leq \phi - \phi_0 \leq 2\pi$. Although the branch of h can be chosen arbitrarily, we require for definiteness that $\operatorname{Im} h < 0$ in the case where the imaginary part of h is nonzero. It is important to emphasize that the obtained distribution constant h of the loop-antenna current exactly coincides with that for a linear strip antenna located at a plane interface of the same media perpendicular to the anisotropy axis of the metamaterial [27]. Hence, for such an orientation of a sufficiently narrow strip conductor of the antenna, the quantity h, which governs the current shape, is independent, in a first approximation, of the curvature of the interface.

It is also worth noting that the limiting cases $\varepsilon_{\rm eff} \to 0$ and $\mu_{\rm eff} \to \infty$, which were supposed to be of little interest, correspond to the vanishing antenna current, as follows from (95). Therefore, a special analysis of these two cases need not be given.

Using (95), it is possible to obtain a simple expression for the input impedance $Z = V_0/I_\Sigma(\phi_0)$ of the antenna:

$$Z = jZ_0\frac{h}{\pi k_0\varepsilon_{\rm eff}}\ln(4a/d)\tan(\pi ha). \quad (96)$$

It is evident that this quantity coincides with the input impedance of a short-circuited transmission line of length πa. Thus, it can be concluded that the approximate results of (95) and (96) correspond to the transmission-line theory for the antenna considered. Interestingly, the current distribution constant h is complex-valued in the case of a hyperbolic metamaterial where the input impedance of the antenna has both the real and imaginary parts within the framework of this theory. In fact, the real part of (96) describes the resonance excitation of waves with hyperbolic dispersion in the limit of vanishing wavelengths. For a nonhyperbolic metamaterial inside the cylinder, the real part of the input impedance can be obtained only if the exact antenna current (94) is used to calculate Z.

If h has a nonzero imaginary part, the input impedance is significantly simplified in the case of an electrically large loop antenna where $\pi|\operatorname{Im} h|a \gg 1$. Under this condition, we get

$$Z = Z_0\frac{h}{\pi k_0\varepsilon_{\rm eff}}\ln(4a/d). \quad (97)$$

This result corresponds to the current distribution which decays with distance from the excitation gap along the strip conductor at a length $|\operatorname{Im} h|^{-1}$ that is much shorter than the antenna radius.

In the opposite case of an electrically small loop where $\pi|h|a \ll 1$, the impedance (96) becomes

$$Z = jZ_0k_0a\mu_{\rm eff}\left[1+\frac{\pi^2}{3}(k_0a)^2\varepsilon_{\rm eff}\mu_{\rm eff}\right]\ln(4a/d). \quad (98)$$

Note that neglecting the small second term in the brackets of (98) is equivalent to taking into account only the uniform part of the current (94) of the loop antenna with a logarithmically narrow strip conductor. If we do this in the case where both normal waves of the metamaterial inside the cylinder have hyperbolic dispersion, the input impedance (98) reduces to

$$Z = Z_0k_0a\frac{2\mu|\mu_\perp\mu_\parallel|^{1/2}}{\mu^2+|\mu_\perp\mu_\parallel|}\left(\mu+j|\mu_\perp\mu_\parallel|^{1/2}\right)\ln(4a/d). \quad (99)$$

In this case, the real part of the impedance (99) is determined by the excitation of waves of the H type, whereas the excitation of waves of the E type gives a negligible contribution to this impedance. If only the H wave of the metamaterial has hyperbolic dispersion, the impedance (99) remains unchanged. However, if only the E wave of the metamaterial has such dispersion, one needs to allow for the imaginary part of the second term in the brackets of (98) to obtain the real part of Z. This leads to

$$Z = Z_0\left[\frac{\pi^2}{6}(k_0a)^3|\varepsilon_\perp\varepsilon_\parallel|^{1/2}\mu_{\rm eff}^2+jk_0a\mu_{\rm eff}\right]\ln(4a/d). \quad (100)$$

The real part of the input impedance (100) is now determined by the contribution of waves of the E type.

B. NUMERICAL RESULTS FOR THE CURRENT DISTRIBUTION AND THE INPUT IMPEDANCE

The principal difficulty encountered in discussing the numerical calculations is that there are many possible combinations of the metamaterial parameters and to give full results for even a few values of each would take up much space. Therefore, we will focus on the behavior of the current distribution and input impedance of the antenna in the most interesting case of a doubly hyperbolic metamaterial inside the cylinder. For our calculations, we took free space as the outer medium ($\varepsilon = \mu = 1$) and chose parameters of the metamaterial so as to satisfy simultaneously the conditions (10) and (11). It was assumed that the angular frequency $\omega = 8.04 \times 10^9$ s^{-1}, the midpoint of the excitation gap has the azimuthal coordinate $\phi_0 = 0$, $\Delta = 0.05$ rad, and $d = 0.02a$. For calculations of the current distribution, the antenna radius a coinciding with the cylinder radius was taken equal to 5 cm.

Fig. 4 shows the normalized (to maximum value) magnitude $|I_\Sigma(\phi)|$ of the antenna current and its phase angle $\theta(\phi) = \arctan[\operatorname{Im} I_\Sigma(\phi)/\operatorname{Re} I_\Sigma(\phi)]$ as functions of the azimuthal angle ϕ for the following values of the tensor elements: $\varepsilon_\perp = -\varepsilon_\parallel = 0.1$ and $\mu_\perp = -\mu_\parallel = 0.1$. In this case, the current distribution constant h is complex-valued such that $ha = (1-j)0.3$. In Fig. 4 and onwards, the solid and dashed lines correspond to the rigorously derived representation (94) and the approximate formula (95) for the antenna current, respectively. We present the current distribution only for the angular interval $0 < \phi < \pi$ since the function $I_\Sigma(\phi)$ is symmetric about the point $\phi = \phi_0 = 0$.

It is seen in Fig. 4 that the current undergoes spatial oscillations decaying with distance from the antenna input. This

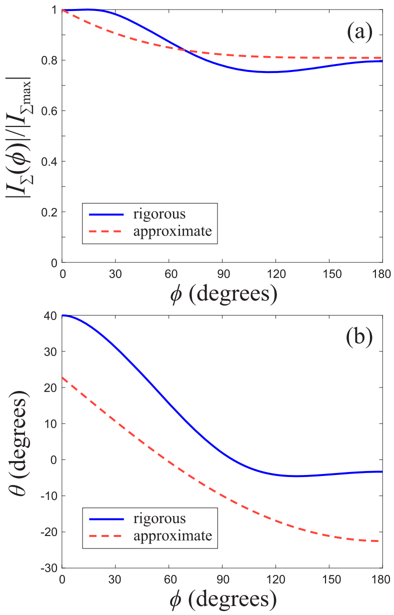

FIGURE 4. (a) Magnitude and (b) phase of the current in an antenna with radius $a = 5$ cm at the frequency $\omega = 8.04 \times 10^9$ s^{-1} for $\varepsilon_\perp = -\varepsilon_\parallel = 0.1$ and $\mu_\perp = -\mu_\parallel = 0.1$ when $ha = (1 - j)0.3$.

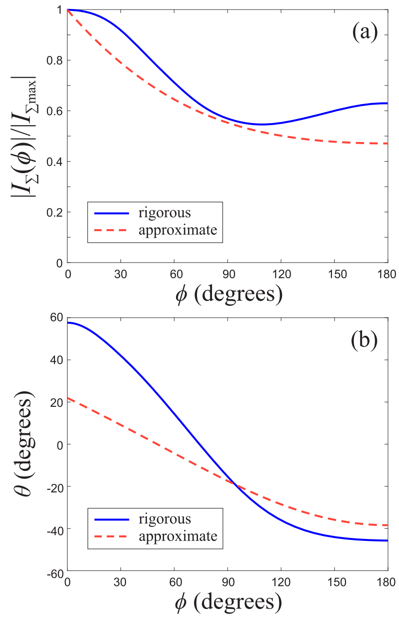

FIGURE 5. Same as in Fig. 4 but for $\varepsilon_\perp = -\varepsilon_\parallel = 0.5$, $\mu_\perp = 0.1$, and $\mu_\parallel = -0.3$ when $ha = 0.35 - j0.47$. (a) Current magnitude. (b) Current phase.

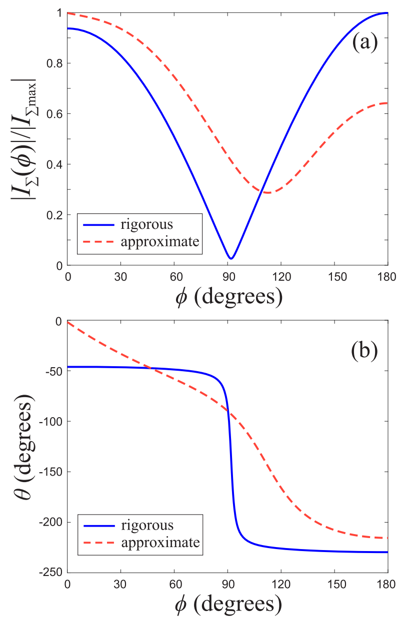

FIGURE 6. Same as in Fig. 4 but with $\mu_\perp$ and $\mu_\parallel$ replaced by $\mu_\perp = -\mu_\parallel = 2$ when $ha = 1.22 - j0.35$. (a) Current magnitude. (b) Current phase.

feature of the current behavior, which corresponds to the complex value of the quantity h, is related to the resonance excitation of the potential waves in the hyperbolic metamaterial cylinder.

Note that the above-mentioned decay of the current magnitude becomes more pronounced if the metamaterial parameters are changed in such a way that the imaginary part of h increases in absolute value. This is illustrated by Fig. 5, which shows the current distribution for $\varepsilon_\perp = -\varepsilon_\parallel = 0.5$, $\mu_\perp = 0.1$, $\mu_\parallel = -0.3$, and the previous values of other parameters. In this case, $ha = 0.35 - j0.47$ and, as a result, a more rapid decay of the current with distance from the excitation gap is observed. However, the dependences in Fig. 5 remain similar to those in Fig. 4.

If the metamaterial parameters are changed to ensure that the real part of h notably exceeds the imaginary part of this quantity in absolute value, then the current magnitude exhibits an oscillatory behavior along the antenna conductor. This is illustrated by Fig. 6 for the same values of $\varepsilon_\perp$ and $\varepsilon_\parallel$ as in Fig. 4 and $\mu_\perp = -\mu_\parallel = 2$. In this case, $ha = 1.22 - j0.35$, and the current attenuation with distance from the excitation gap is less pronounced.

It also follows from comparison of the rigorous and approximate results for the current distributions in Figs. 4–6 that the simple approximate formula (95) adequately describes the general features of the current distribution. This takes place despite the fact that the logarithm $\ln(4a/d)$ is greater than $|S_m|$ with a moderate margin for the used parameters. Although the solid and dashed curves in these figures could be made closer by increasing $\ln(4a/d)$, this would result in such a small width of the antenna strip conductor that seems not applicable for realistic values of a and d. Nevertheless, knowing the value of the quantity h, we can always predict qualitatively the shape of the current distribution. Thus, for a purely real h, we will have an oscillatory current distribution coinciding with that for the same antenna immersed in a conventional isotropic medium with the refractive index $\sqrt{\varepsilon_{\text{eff}}\mu_{\text{eff}}}$. For a purely imaginary h, the current magnitude will exponentially decay near the excitation gap with distance from it. Since the current distributions

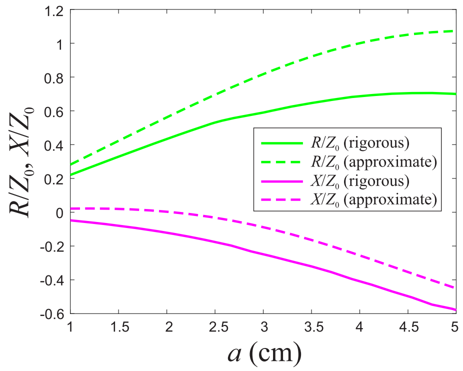

FIGURE 7. Real (*R*) and imaginary (*X*) parts of the input impedance as functions of the antenna radius *a*. Same values of other parameters as in Fig. 4.

are rather evident in these two cases, we do not present here the corresponding numerical results for the sake of brevity.

As for the antenna input impedance $Z = R + jX$, its real and imaginary parts are shown in Fig. 7 as functions of the antenna radius a for the same values of other parameters as in Fig. 4. The solid and dashed lines in Fig. 7 correspond to the rigorous result for Z and the approximate formula (96), respectively. Fig. 7 demonstrates an interesting feature that in the case of a thin-wire antenna with moderate radius, the quantity R can be higher than the input reactance X in absolute value. This is explained by the efficient excitation of the potential waves with hyperbolic dispersion inside the cylinder. Due to this fact, the curves in Fig. 7 do not demonstrate any resonance features. We do not present here the frequency dependences for the antenna impedance, which would require consideration of the dispersive properties of particular metamaterials. Such analysis will be performed elsewhere.

VI. CONCLUSION

In this article, we have analyzed the problem of the current distribution and input impedance of a loop antenna located on the surface of a uniaxial metamaterial cylinder surrounded by an isotropic magnetodielectric. Using a full-wave formulation, we have derived and solved integral equations for azimuthal harmonics of the antenna current in all possible cases that can be encountered for the material parameters of the considered media. For the corresponding integral equations, we have rigorously calculated the singular parts of the kernels and approximated their regular parts in the case of a sufficiently narrow strip conductor of the antenna. Then the resulting integral equations have been solved exactly, and the closed-form representations for the antenna characteristics have been obtained. It has been demonstrated that these characteristics are determined by some effective dielectric and magnetic parameters, which admit relatively simple representations. In view of this, there is a reason to believe that our approach can be used in treating similar problems with more complicated material parameters.

Although the results of the presented analysis can be used for determining other characteristics of the discussed antenna, including the radiation pattern in the surrounding medium and the field distribution inside the metamaterial cylinder, these topics fall beyond the scope of this article and will be considered elsewhere. Since our consideration has been made for a very narrow strip, future work should also be focused on the determination of the conditions under which the developed theory can be suitable for wider strips. An effort toward such an analysis, which requires direct numerical simulations based on rather complicated computational techniques [44], [45], can provide a more general appraisal of this theory.

APPENDIX A
PROPAGATING MODES OF THE HYPERBOLIC METAMATERIAL CYLINDER

It can be shown that under conditions (10) and (11), the metamaterial cylinder supports an infinitely large number of eigenmodes of the E and H types. The propagation constants $p_{m,n}$ of these modes are determined by the dispersion relation (33) and tend to infinity with increasing n. It can be verified that the left-hand side of this relation is independent of the sign of m. With allowance for this fact, it follows that, in the limit $|p_{m,n}| \to \infty$, (33) splits into the separate relations for the E and H modes:

$$\frac{J_{|m|+1}(k_0 a q_1)}{J_{|m|}(k_0 a q_1)} = \frac{\varepsilon\sigma_1}{|\varepsilon_\perp \varepsilon_\parallel|^{1/2}} \tag{101}$$

$$\frac{J_{|m|+1}(k_0 a q_2)}{J_{|m|}(k_0 a q_2)} = \frac{\mu\sigma_2}{|\mu_\perp \mu_\parallel|^{1/2}}. \tag{102}$$

Here, $q_1 = \gamma_1\sigma_1 p^{(1)}_{m,n}$ and $q_2 = \gamma_2\sigma_2 p^{(2)}_{m,n}$, where the quantities $p^{(1)}_{m,n}$ and $p^{(2)}_{m,n}$ denote the propagation constants of the E and H modes and are found from (101) and (102), respectively. Other notations in (101) and (102) are the same as in (56). We denote the transverse wavenumber q in the outer region of the cylinder as $q^{(1)}$ and $q^{(2)}$ for the E and H modes, respectively. Then, in the limiting case considered here, it can be shown that $q^{(1,2)} = -j\sigma_{1,2} p^{(1,2)}_{m,n}$. In the interests of brevity, when writing the transverse wavenumbers for the inner and outer regions of the metamaterial cylinder, we omit the subscripts m and n.

Since the propagation constants are assumed relatively large in magnitude such that $k_0 a|q_{1,2}| \gg 1$, one can use the large-argument approximation for the Bessel functions in (101) and (102) to arrive at

$$p^{(1,2)}_{m,n} = \frac{1}{k_0 a \gamma_{1,2}}\left[\tau_{1,2} + \frac{\pi\sigma_{1,2}}{2}(2n + |m| + 1/2)\right] \tag{103}$$

where

$$\tau_1 = \arctan\frac{\varepsilon}{|\varepsilon_\perp \varepsilon_\parallel|^{1/2}}, \quad \tau_2 = \arctan\frac{\mu}{|\mu_\perp \mu_\parallel|^{1/2}}$$

and n is a sufficiently large positive integer. Note that the positive and negative values of $p^{(1,2)}_{m,n}$ for $n > 0$ refer to the forward and backward modes, respectively.

For $|p^{(1)}_{m,n}| \to \infty$, the fields of the E modes are described to a good approximation by the formulas which can be obtained from the rigorous expressions by putting $\mathcal{B}_{m,n} = 0$ and

$\mathcal{D}_{m,n} = 0$. Then, we can obtain from (20) the following approximate expressions for the dominant field components of these modes in the region $\rho < a$:

$$E_{\rho;m,n}(\rho) = -\frac{p^{(1)}_{m,n}}{\varepsilon_\perp} J_{m+1}(k_0 q_1 \rho)\mathcal{A}_{m,n}$$
$$E_{z;m,n}(\rho) = j\frac{q_1}{\varepsilon_\parallel} J_m(k_0 q_1 \rho)\mathcal{A}_{m,n}$$
$$H_{\phi;m,n}(\rho) = -Z_0^{-1} J_{m+1}(k_0 q_1 \rho)\mathcal{A}_{m,n}. \quad (104)$$

In this limiting case, the azimuthal electric field of the E modes is written as

$$E_{\phi;m,n}(\rho) = -j\frac{p^{(1)}_{m,n}}{\varepsilon_\perp} m \frac{J_m(k_0 q_1 \rho)}{k_0 q_1 \rho}\mathcal{A}_{m,n}. \quad (105)$$

The corresponding field expressions for the region $\rho > a$ are obtained from (104) and (105) by taking the second-kind Hankel functions instead of the Bessel functions [see (21)] and making the replacements $\mathcal{A}_{m,n} \to \mathcal{C}_{m,n}$, $q_1 \to q^{(1)}$, and $\varepsilon_{\perp,\parallel} \to \varepsilon$. The relation between the mode coefficients $\mathcal{A}_{m,n}$ and $\mathcal{C}_{m,n}$ is determined from the continuity condition for the longitudinal component of the electric field at $\rho = a$. It can be verified that the electric field of the considered E modes is expressible as $\mathbf{E}_{m,n} = -\nabla\varphi^{(e)}_{m,n}$, where $\varphi^{(e)}_{m,n}$ is the electric scalar potential. Hence, such modes may be called electrostatic. Then it can be found that the norms $N^{(1)}_{m,n}$ of the electrostatic E modes are determined by integration of the term $E_{\rho;m,n}H_{\phi;m,n}$, which is predominant in the integrand of (38). Moreover, a close examination shows that it is sufficient to integrate this term between the limits $\rho = 0$ and $\rho = a$ since the integration over the region $\rho > a$ gives a negligible contribution to $N^{(1)}_{m,n}$. Thus, we get

$$N^{(1)}_{m,n} = \frac{4\pi}{Z_0}\frac{p^{(1)}_{m,n}}{\varepsilon_\perp}\mathcal{A}^2_{m,n}\int_0^a J^2_{m+1}(k_0 q_1 \rho)\rho d\rho. \quad (106)$$

Evaluating the integral in (106) in the limit $|p^{(1)}_{m,n}| \to \infty$ [39] and taking into account the relation (101), we obtain

$$N^{(1)}_{m,n} = \frac{2\pi}{Z_0}\frac{p^{(1)}_{m,n}}{\varepsilon_\perp}\frac{\varepsilon_u^2 - \varepsilon^2}{\varepsilon_u^2}\mathcal{A}^2_{m,n} a^2 J^2_m(k_0 a q_1). \quad (107)$$

Let us now proceed to the H modes. In the case $|p^{(2)}_{m,n}| \to \infty$, their fields are approximately described by putting $\mathcal{A}_{m,n} = 0$ and $\mathcal{C}_{m,n} = 0$, and the dominant field components of these modes for $\rho < a$ are written as

$$E_{\phi;m,n}(\rho) = jJ_{m+1}(k_0 q_2 \rho)\mathcal{B}_{m,n}$$
$$H_{\rho;m,n}(\rho) = -jZ_0^{-1}\frac{p^{(2)}_{m,n}}{\mu_\perp} J_{m+1}(k_0 q_2 \rho)\mathcal{B}_{m,n}$$
$$H_{z;m,n}(\rho) = -Z_0^{-1}\frac{q_2}{\mu_\parallel} J_m(k_0 q_2 \rho)\mathcal{B}_{m,n}. \quad (108)$$

The field components of the H modes in the region $\rho > a$ are obtained from (108) similarly to the E modes, but now, along with the use of the Hankel functions instead of the Bessel functions, one should make the replacements $\mathcal{B}_{m,n} \to \mathcal{D}_{m,n}$, $q_2 \to q^{(2)}$, and $\mu_{\perp,\parallel} \to \mu$. The relation between the coefficients $\mathcal{B}_{m,n}$ and $\mathcal{D}_{m,n}$ is determined from the continuity condition for the longitudinal component of the magnetic field at $\rho = a$. Here, by analogy with the E modes, the H modes may be called magnetostatic since their magnetic field is expressible via the magnetic scalar potential $\varphi^{(m)}_{m,n}$ as $\mathbf{H}_{m,n} = -\nabla\varphi^{(m)}_{m,n}$. It can also be found that the norms $N^{(2)}_{m,n}$ of the magnetostatic H modes are determined by integration of the term $E_{\phi;m,n}H_{\rho;m,n}$ between the limits $\rho = 0$ and $\rho = a$. This gives

$$N^{(2)}_{m,n} = \frac{4\pi}{Z_0}\frac{p^{(2)}_{m,n}}{\mu_\perp}\mathcal{B}^2_{m,n}\int_0^a J^2_{m+1}(k_0 q_2 \rho)\rho d\rho. \quad (109)$$

Evaluating the integral in (109) at $|p^{(2)}_{m,n}| \to \infty$ and making use of (102), we get

$$N^{(2)}_{m,n} = \frac{2\pi}{Z_0}\frac{p^{(2)}_{m,n}}{\mu_\perp}\frac{\mu_u^2 - \mu^2}{\mu_u^2}\mathcal{B}^2_{m,n} a^2 J^2_m(k_0 a q_2). \quad (110)$$

Calculating the field component $E_{\phi;m,n}$ of the E and H modes and allowing for (107) and (110), we arrive at (55) with the series defined by (56). When doing this, we neglect the bounded terms $\tau_{1,2}$, which are present in (103). In the exponential function of (56), this can be made by virtue of the first two conditions in (46).

The series in (67) is derived using the $E_{\phi;m,n}$ and $E_{z;m,n}$ components of the E modes in a similar way, but with allowance for a small collisional loss in the metamaterial by inserting an infinitesimal term ν in the exponential function of the series in (67). This ensures convergence of this series, with further passage to the weak limit $\nu \to 0$.

APPENDIX B
EVALUATION OF SOME SINGULAR INTEGRALS

Using the large-argument asymptotics for the modified Bessel functions, we can rewrite the singular integrals (75) and (76) as

$$\tilde{I}^{(1)}_m = \frac{2\pi k_0 a \gamma_1}{\alpha_1(1+\alpha_1)}\hat{I}^{(1)}_m + \delta\tilde{I}^{(1)}_m \quad (111)$$
$$\tilde{I}^{(2)}_m = \frac{2\pi k_0 a \gamma_2}{1+\alpha_2}\hat{I}^{(2)}_m + \delta\tilde{I}^{(2)}_m \quad (112)$$

where

$$\hat{I}^{(1,2)}_m = \int_0^\infty I^2_{|m|}(k_0 a\gamma_{1,2}\tilde{p})\cos(k_0\zeta\tilde{p})\exp(-2k_0 a\gamma_{1,2}\tilde{p})d\tilde{p} \quad (113)$$

and $\delta\tilde{I}^{(1)}_m$ and $\delta\tilde{I}^{(2)}_m$ are the regular quantities. These quantities, which may be taken at $\zeta = 0$, account for the difference between (75) and (76), on the one hand, and their respective approximations given by the first terms in (111) and (112), on the other hand. Each of the integrals in (113) can be evaluated in closed form as the following limit with an infinitesimal λ [39]:

$$\hat{I}^{(1,2)}_m = \mathrm{Re}\lim_{\lambda\to 0}\int_0^\infty I^2_{|m|}(k_0 a\gamma_{1,2}\tilde{p}) \times \exp[-(\lambda + 2k_0 a\gamma_{1,2} + jk_0|\zeta|)\tilde{p}]d\tilde{p}$$

$$= \frac{1}{\pi k_0 a\gamma_{1,2}} \mathrm{Re} \lim_{\lambda\to 0} Q_{|m|-\frac{1}{2}} \left(\frac{\Lambda^2}{2(k_0 a\gamma_{1,2})^2} - 1 \right) \quad (114)$$

where $\Lambda = \lambda + 2k_0 a\gamma_{1,2} + jk_0|\zeta|$. Since the argument of the Legendre function in (114) is close to unity, we can approximate this function as described in [40]. This approximation leads to (77) and (78).

APPENDIX C
COMPLEX MODES OF THE NONHYPERBOLIC METAMATERIAL CYLINDER

As was noted above, the E and H complex eigenmodes are supported by the nonhyperbolic metamaterial cylinder under the conditions $\mathrm{sgn}\,\varepsilon \neq \mathrm{sgn}\,\varepsilon_u$ and $\mathrm{sgn}\,\mu \neq \mathrm{sgn}\,\mu_u$, respectively. For sufficiently large magnitudes of the complex propagation constants of such modes, their dispersion relation takes the form

$$\frac{J_{|m|+1}(k_0 a q_{1,2})}{J_{|m|}(k_0 a q_{1,2})} = -j\alpha_{1,2}. \quad (115)$$

As previously, the subscripts 1 and 2 in (115) refer to the complex modes of the E and H types with the propagation constants $p^{(1)}_{m,n}$ and $p^{(2)}_{m,n}$, respectively. For the complex modes of both types, the transverse wavenumbers in the inner and outer regions of the metamaterial cylinder are related as $q_{1,2} = \gamma_{1,2} q^{(1,2)}$ in the limit $|p^{(1,2)}_{m,n}| \to \infty$. Moreover, for each type, two families of the complex modes exist. This is related to the fact that if the propagation constant $p^{(1,2)}_{m,n}$, which corresponds to the transverse wavenumber $q^{(1,2)}$ in the outer region, is a complex-valued solution of (115), then $-(p^{(1,2)}_{m,n})^*$, which corresponds to $-(q^{(1,2)})^*$, is also a solution. A careful examination of (115) in the large-argument approximation for cylindrical functions shows that, in the limit $|p^{(1,2)}_{m,n}| \to \infty$, one obtains $q^{(1,2)} = jp^{(1,2)}_{m,n}$ for the first family of the complex modes, with

$$p^{(1,2)}_{m,n} = \frac{1}{k_0 a\gamma_{1,2}} \left[\xi^{(1,2)}_k - j\frac{\pi}{2}(2n + |m| + 1/2) \right] \quad (116)$$

where $k = 1$ and the definition of $\xi^{(1,2)}_k$ is given by (82). For the second family of the complex modes, we have $q^{(1,2)} = -jp^{(1,2)}_{m,n}$, where $p^{(1,2)}_{m,n}$ is again given by (116), but with $k = 2$.

Interestingly, the complex modes of the E type turn out to be electrostatic in the considered limiting case. It can be verified by straightforward manipulation that expressions (104)–(107) remain formally valid for the complex modes of this type if one takes the propagation constants $p^{(1)}_{m,n}$ given by (116) for the first or second family of the corresponding mode solutions. Similarly, the complex modes of the H type turn out to be magnetostatic. For them, expressions (108)–(110) may be used if the propagation constants $p^{(2)}_{m,n}$ of (116) for the first or second family of these modes are taken.

Thus, the calculation of the contribution from the complex modes to the kernels of the integral equations is similar to that for the propagating modes discussed in Appendix A, with the only significant difference consisting in the necessity to take into account two families of the complex modes, which is provided by the summation over k in (81) and (85).

REFERENCES

[1] D. R. Smith and D. Schurig, "Electromagnetic wave propagation in media with indefinite permittivity and permeability tensors," *Phys. Rev. Lett.*, vol. 90, no. 7, Feb. 2003, Art. no. 077405.

[2] J. B. Pendry, D. Schurig, and D. R. Smith, "Controlling electromagnetic fields," *Science*, vol. 312, pp. 1780–1782, Jun. 2006.

[3] L. M. Custodio, C. T. Sousa, J. Ventura, J. M. Teixeira, P. V. S. Marques, and J. P. Araujo, "Birefringence swap at the transition to hyperbolic dispersion in metamaterials," *Phys. Rev. B, Condens. Matter*, vol. 85, no. 16, Apr. 2012, Art. no. 165408.

[4] A. Poddubny, I. Iorsh, P. Belov, and Y. Kivshar, "Hyperbolic metamaterials," *Nature Photon.*, vol. 7, no. 12, pp. 948–957, Dec. 2013.

[5] P. Shekhar, J. Atkinson, and Z. Jacob, "Hyperbolic metamaterials: Fundamentals and applications," *Nano Converg.*, vol. 1, no. 1, p. 14, Jun. 2014.

[6] I. S. Nefedov and S. A. Tretyakov, "Waveguide containing a backward-wave slab," *Radio Sci.*, vol. 38, no. 6, pp. 1101–1110, Dec. 2003.

[7] I. V. Shadrivov, A. A. Sukhorukov, and Y. S. Kivshar, "Guided modes in negative-refractive-index waveguides," *Phys. Rev. E, Stat. Phys. Plasmas Fluids Relat. Interdiscip. Top.*, vol. 67, no. 5, May 2003, Art. no. 057602.

[8] B.-I. Wu, T. M. Grzegorczyk, Y. Zhang, and J. A. Kong, "Guided modes with imaginary transverse wave number in a slab waveguide with negative permittivity and permeability," *J. Appl. Phys.*, vol. 93, no. 11, pp. 9386–9388, Jun. 2003.

[9] C. M. Krowne, "Electromagnetic-field theory and numerically generated results for propagation in left-handed guided-wave single-microstrip structures," *IEEE Trans. Microw. Theory Techn.*, vol. 51, no. 12, pp. 2269–2283, Dec. 2003.

[10] A. Alù and N. Engheta, "Guided modes in a waveguide filled with a pair of single-negative (SNG), double-negative (DNG), and/or double-positive (DPS) layers," *IEEE Trans. Microw. Theory Techn.*, vol. 52, no. 1, pp. 199–210, Jan. 2004.

[11] G. Minatti, F. Caminita, E. Martini, M. Sabbadini, and S. Maci, "Synthesis of modulated-metasurface antennas with amplitude, phase, and polarization control," *IEEE Trans. Antennas Propag.*, vol. 64, no. 9, pp. 3907–3919, Sep. 2016.

[12] A. C. Tasolamprou *et al.*, "Exploration of intercell wireless millimeter-wave communication in the landscape of intelligent metasurfaces," *IEEE Access*, vol. 7, pp. 122931–122948, 2019.

[13] A. Alù and N. Engheta, "Radiation from a traveling-wave current sheet at the interface between a conventional material and a metamaterial with negative permittivity and permeability," *Microw. Opt. Technol. Lett.*, vol. 35, no. 6, pp. 460–463, Nov. 2002.

[14] A. Alù, M. G. Silveirinha, A. Salandrino, and N. Engheta, "Epsilon-near-zero metamaterials and electromagnetic sources: Tailoring the radiation phase pattern," *Phys. Rev. B, Condens. Matter*, vol. 75, no. 15, Apr. 2007, Art. no. 155410.

[15] P. Baccarelli *et al.*, "Effects of leaky-wave propagation in metamaterial grounded slabs excited by a dipole source," *IEEE Trans. Microw. Theory Techn.*, vol. 53, no. 1, pp. 32–44, Jan. 2005.

[16] G. Lovat, P. Burghignoli, F. Capolino, D. R. Jackson, and D. R. Wilton, "Analysis of directive radiation from a line source in a metamaterial slab with low permittivity," *IEEE Trans. Antennas Propag.*, vol. 54, no. 3, pp. 1017–1030, Mar. 2006.

[17] A. N. Askarpour and P. L. E. Uslenghi, "Exact dipole radiation from an oblate semi-spheroidal cavity filled with DNG metamaterial," *IEEE Trans. Antennas Propag.*, vol. 59, no. 7, pp. 2473–2479, Jul. 2011.

[18] K. G. Balmain, A. A. E. Lüttgen, and P. C. Kremer, "Resonance cone formation, reflection, refraction, and focusing in a planar anisotropic metamaterial," *IEEE Antennas Wireless Propag. Lett.*, vol. 1, pp. 146–149, 2002.

[19] Y. You, "Radiation from a current sheet at the interface between a conventional medium and anisotropic negative refractive medium," *Bull. Mater. Sci.*, vol. 32, no. 4, pp. 437–441, Aug. 2009.

[20] O. Kidwai, S. V. Zhukovsky, and J. E. Sipe, "Dipole radiation near hyperbolic metamaterials: Applicability of effective-medium approximation," *Opt. Lett.*, vol. 36, pp. 2530–2532, Jul. 2011.

[21] D. S. Filonov, A. S. Shalin, I. Iorsh, P. A. Belov, and P. Ginzburg, "Controlling electromagnetic scattering with wire metamaterial resonators," *J. Opt. Soc. Amer. A, Opt. Image Sci.*, vol. 33, no. 10, pp. 1910–1916, Oct. 2016.

[22] F. Costa, O. Luukkonen, C. R. Simovski, A. Monorchio, S. A. Tretyakov, and P. M. de Maagt, "TE surface wave resonances on high-impedance surface based antennas: Analysis and modeling," *IEEE Trans. Antennas Propag.*, vol. 59, no. 10, pp. 3588–3596, Oct. 2011.

[23] I. S. Nefedov and S. A. Tretyakov, "On potential applications of metamaterials for the design of broadband phase shifters," *Microw. Opt. Technol. Lett.*, vol. 45, no. 2, pp. 98–102, Apr. 2005.

[24] D. Pozar, "Radiation and scattering from a microstrip patch on a uniaxial substrate," *IEEE Trans. Antennas Propag.*, vol. 35, no. 6, pp. 613–621, Jun. 1987.

[25] K. Li, S.-O. Park, H. Lee, J. Ma, B.-C. Kim, and H.-D. Choi, "Analytical technique to evaluate the asymptotic part of the impedance matrix of microstrip dipole on a uniaxial substrate," *Prog. Electromagn. Res.*, vol. 35, pp. 127–139, 2002.

[26] F. Bilotti, L. Vegni, and A. Toscano, "Radiation and scattering features of patch antennas with bianisotropic substrates," *IEEE Trans. Antennas Propag.*, vol. 51, no. 3, pp. 449–456, Mar. 2003.

[27] A. V. Kudrin, T. M. Zaboronkova, A. S. Zaitseva, and B. Spagnolo, "Theory of a strip antenna located at a plane interface of a uniaxial metamaterial and an isotropic magnetodielectric," *IEEE Trans. Antennas Propag.*, vol. 68, no. 1, pp. 195–206, Jan. 2020.

[28] A. V. Kudrin, A. S. Zaitseva, T. M. Zaboronkova, and S. S. Zilitinkevich, "Current distribution and input impedance of a strip loop antenna located on the surface of a circular column filled with a resonant magnetoplasma," *Prog. Electromagn. Res. B*, vol. 55, pp. 241–256, 2013.

[29] T. M. Zaboronkova, A. S. Zaitseva, A. V. Kudrin, and O. S. Mukhina, "Theory of a circular loop antenna located on the surface of a dielectric column in a magnetoplasma," *Radiophys. Quantum Electron.*, vol. 59, no. 12, pp. 1000–1016, Jun. 2017.

[30] A. V. Kudrin, T. M. Zaboronkova, A. S. Zaitseva, and C. Krafft, "Electrodynamic characteristics of a loop antenna located on the surface of a uniaxial anisotropic cylinder," in *Proc. Days Diffraction (DD)*, St. Petersburg, Russia, Jun. 2016, pp. 253–258.

[31] A. V. Kudrin, A. S. Zaitseva, T. M. Zaboronkova, and C. Krafft, "Current distribution and input impedance of a circular loop antenna located on the surface of a gyromagnetic cylinder," in *Proc. Days Diffraction (DD)*, St. Petersburg, Russia, Jun. 2018, pp. 192–197.

[32] A. S. Zaitseva, A. V. Kudrin, and T. M. Zaboronkova, "Analysis of a circular loop antenna located on a hyperbolic metamaterial cylinder," in *Proc. 3rd URSI Atlantic Asia Pacific Radio Sci. Meeting (AT-AP-RASC)*, Gran Canaria, Spain, May 2022, pp. 1–4.

[33] G. W. Milton, "Realizability of metamaterials with prescribed electric permittivity and magnetic permeability tensors," *New J. Phys.*, vol. 12, no. 3, Mar. 2010, Art. no. 033035.

[34] L. B. Felsen and N. Marcuvitz, *Radiation and Scattering of Waves*. Hoboken, NJ, USA: Wiley, 2003.

[35] J. A. Kong, *Electromagnetic Wave Theory*. Cambridge, MA, USA: EMW Publishing, 2005.

[36] T. Tamir and A. A. Oliner, "The spectrum of electromagnetic waves guided by a plasma layer," *Proc. IEEE*, vol. 51, no. 2, pp. 317–332, Feb. 1963.

[37] V. V. Shevchenko, *Continuous Transitions in Open Waveguides*. Boulder, CO, USA: Golem, 1971.

[38] I. G. Kondrat'ev, A. V. Kudrin, and T. M. Zaboronkova, *Electrodynamics of Density Ducts in Magnetized Plasmas*. Amsterdam, The Netherlands: Gordon & Breach, 1999.

[39] A. P. Prudnikov, Y. A. Brychkov, and O. I. Marichev, *Integrals and Series*, vol. 2. Amsterdam, The Netherlands: Gordon & Breach, 1998.

[40] A. Erdélyi, W. Magnus, F. Oberhettinger, and F. G. Tricomi, *Higher Transcendental Functions*, vol. 1. New York, NY, USA: McGraw-Hill, 1953.

[41] I. S. Gradshteyn and I. M. Ryzhik, *Tables of Integrals, Series, and Products*, 7th ed. New York, NY, USA: Academic, 2007.

[42] F. D. Gakhov, *Boundary Value Problems*. Oxford, U.K.: Pergamon, 1966.

[43] J. Meixner, "The behavior of electromagnetic fields at edges," *IEEE Trans. Antennas Propag.*, vol. AP-20, no. 4, pp. 442–446, Jul. 1972.

[44] E. A. Shirokov, "Application of the method of moments for calculating electrodynamic characteristics of a quasistatic antenna in an anisotropic medium," *Radiophys. Quantum Electron.*, vol. 61, no. 5, pp. 350–361, Oct. 2018.

[45] L. He, T. He, H. R. Zeng, and K. Li, "Current distribution and input impedance of a VLF tubular antenna in a cold plasma," *IEEE Access*, vol. 8, pp. 135347–135356, 2020.

ANNA S. ZAITSEVA received the M.Sc. and Ph.D. degrees in radio physics from the University of Nizhny Novgorod, Nizhny Novgorod, Russia, in 2010 and 2013, respectively, and the Ph.D. degree in applied physics from the University of Palermo, Palermo, Italy, in 2015.

Since 2015, she has been with the Department of Radiophysics, University of Nizhny Novgorod, where she is currently an Associate Professor. Her current research interests include antenna theory in anisotropic and gyrotropic media, open waveguides, and electromagnetic radiation from antennas in plasmas.

Dr. Zaitseva was a recipient of the URSI Commission B Young Scientist Award at the International Symposium on Electromagnetic Theory, Hiroshima, Japan, in 2013, and the URSI Young Scientist Award at the XXXIst General Assembly and Scientific Symposium of the International Union of Radio Science (URSI GASS), Beijing, China, in 2014.

ALEXANDER V. KUDRIN received the M.Sc. (Hons.), Ph.D., and D.Sc. degrees in radio physics from the University of Nizhny Novgorod, Nizhny Novgorod, Russia, in 1987, 1994, and 2004, respectively.

Since 1987, he has been with the Department of Radiophysics, University of Nizhny Novgorod, where he is currently a Full Professor. Since 2007, he has been the Head of the Electrodynamics Division, University of Nizhny Novgorod. He has authored more than 190 articles in peer-reviewed journals and conference proceedings. His current research interests include open waveguides in anisotropic media, antenna theory and wave propagation in plasmas, and electromagnetic waves in nonlinear media.

Dr. Kudrin is a member of the Editorial Board of *Radiophysics and Quantum Electronics* and the Russian National Committee of the International Union of Radio Science (URSI) Commissions B and H. He is a Certified Expert of the Russian Academy of Sciences and an Expert of the Russian Science Foundation.

TATYANA M. ZABORONKOVA received the M.Sc. (Hons.) and Ph.D. degrees in radio physics from the University of Nizhny Novgorod, Nizhny Novgorod, Russia, in 1970 and 1979, respectively, and the D.Sc. degree in radio physics from the Radiophysical Research Institute, Nizhny Novgorod, in 1994.

She was a Visiting Professor with École Polytechnique, Palaiseau, France. Since 1970, she has been with the Radiophysical Research Institute. Since 1985, she has been with the Department of Nuclear Physics, R. E. Alekseev Technical University of Nizhny Novgorod, Nizhny Novgorod, where she is currently a Full Professor. Since 2020, she has also been a Research Fellow with the Department of Radiophysics, University of Nizhny Novgorod. She has authored more than 200 articles in peer-reviewed journals and conference proceedings. Her current research interests include plasma physics, antenna theory, and the nonlinear theory of diffraction of electromagnetic waves.